West Pomeranian University of Technology in Szczecin

Thermal-hydraulic problems in superconducting cables for fusion technology

dr hab. inż. Monika LEWANDOWSKA, prof. ZUT

IFJ PAN

West Pomeranian University of Technology in Szczecin

IFJ PAN Seminar, 5 October 2023

Outline

- Introduction
  - Nuclear fusion
  - Magnetic confinement of plasma
  - ITER and EU-DEMO projects
  - Magnet system of a fusion reactor
  - Critical Surface and thermal stability of superconductors
  - Designs of superconducting coils of EU-DEMO
- Thermal – hydraulic problems in superconducting cables for fusion
  - Simulations (tools, input data, typical results)
  - Experimental research
- Summary

Nuclear fusion - energy source of stars

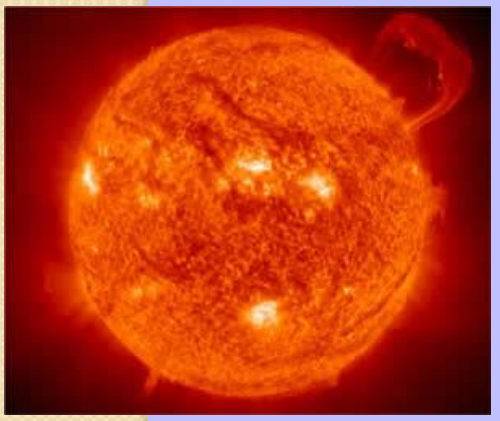

pp

$p^+ + p^+ \rightarrow {}^2H + e^+ + \nu_e$

99,77 %

0,23 %

pep

$p^+ + e^- + p^+ \rightarrow {}^2H + \nu_e$

10^{-5} %

84,92 %

$^2H + p^+ \rightarrow {}^3He + \gamma$

$^3He + p^+ \rightarrow {}^4He + e^+ + \nu_e$

hep

15,08 %

$^3He + {}^4He \rightarrow {}^7Be + \gamma$

0,1 %

99,9 %

^7Be

$^7Be + e^- \rightarrow {}^7Li + \nu_e$

$^7Be + p^+ \rightarrow {}^8B + \gamma$

^8B

$^3He + {}^3He \rightarrow {}^4He + 2p^+$

ppI

$^7Li + p^+ \rightarrow {}^4He + {}^4He$

ppII

$^8B \rightarrow {}^8Be^* + e^+ + \nu_e$

$^8Be^* \rightarrow {}^4He + {}^4He$

ppIII

p-p chain reactions

Fusion reactions of interest

$$D + T \rightarrow {}^{4}He\ (3.5\ MeV) + n\ (14.1\ MeV)$$

$$D + D \rightarrow {}^{3}He\ (0.82\ MeV) + n\ (2.45\ MeV)$$

$$D + D \rightarrow T\ (1.01\ MeV) + H\ (3.02\ MeV)$$

$$D + {}^{3}He \rightarrow {}^{4}He\ (3.6\ MeV) + H\ (14.7\ MeV)$$

Reactions for breeding tritium

(Natural lithium = 7.42 % ^{6}Li and 92.58 % ^{7}Li)

$$^{7}Li + n \rightarrow {}^{4}He + T + n - 2.47\ MeV$$

$$^{6}Li + n \rightarrow {}^{4}He\ (2.05\ MeV) + T\ (2.73\ MeV)$$

Plasma ignition conditions

In a burning plasma a sufficient number of particles must collide with one another with sufficient frequency and intensity.

Plasma density n : ~ 10^{20} m^{-3} (~1 mg/m^3)

Plasma temperature T : at least 100 MK

Energy confinement time τ_E : ~ 2 s

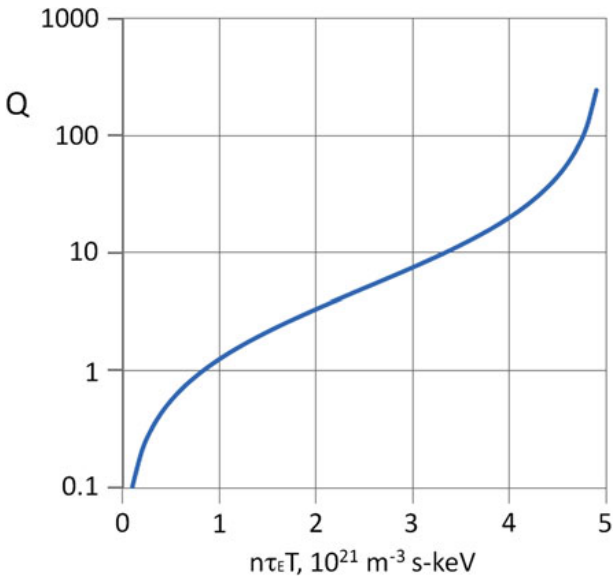

A fusion reactor requires values of the
triple product $n \cdot T \cdot \tau_E > 3 \cdot 10^{21}$ m^{-3} keV s

Energy gain ratio:
Q = (fusion power) / (input power)

in the core of Sun:
15 MK
153 000 kg/m^3

https://www.ipp.mpg.de/15144/zuendbedingungen

Progress toward fusion energy (I)

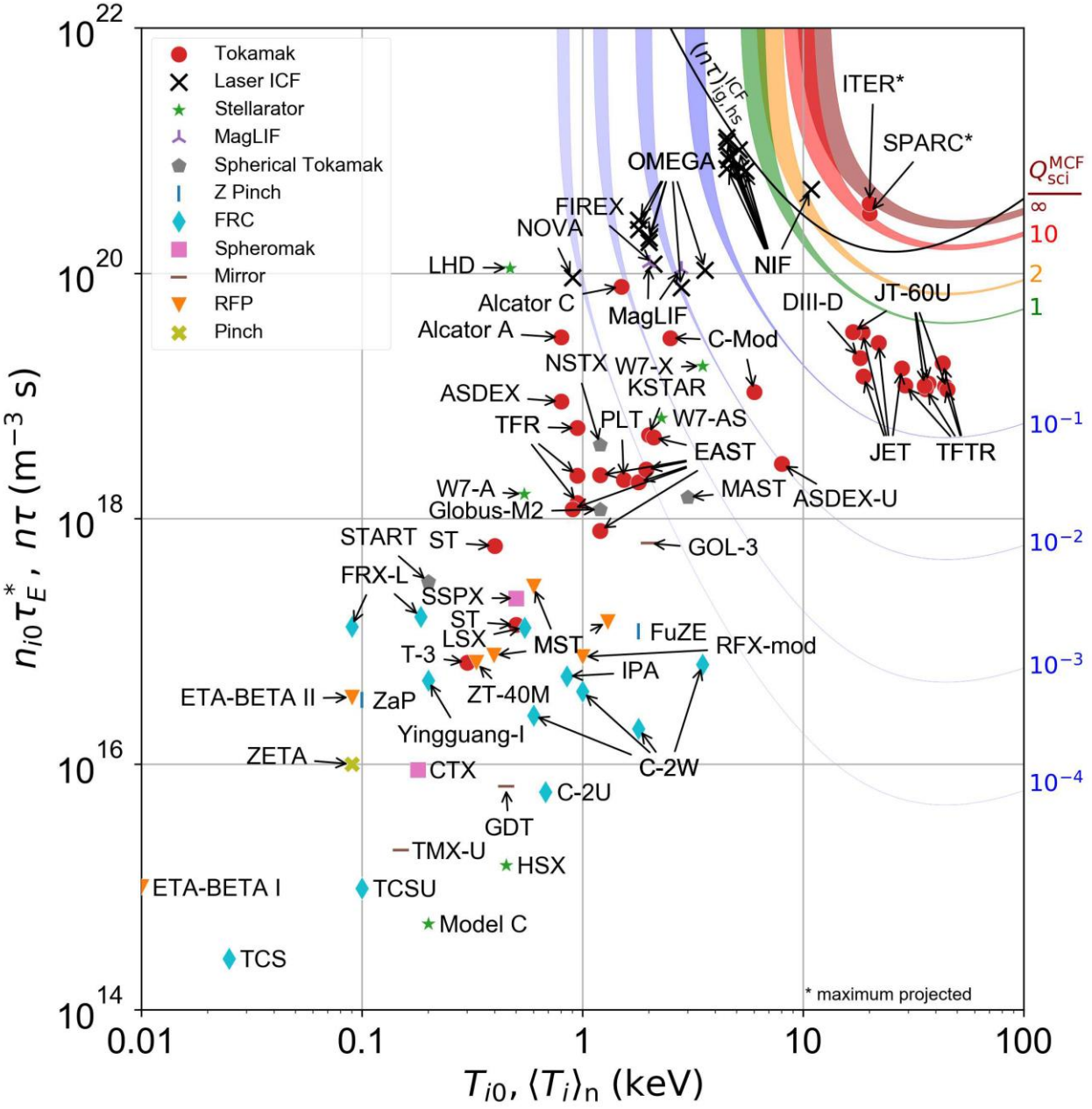

SE Wurzel, S.C. Hsu, Phys. Plasmas 29 (2022) 062103

Progress toward fusion energy (II)

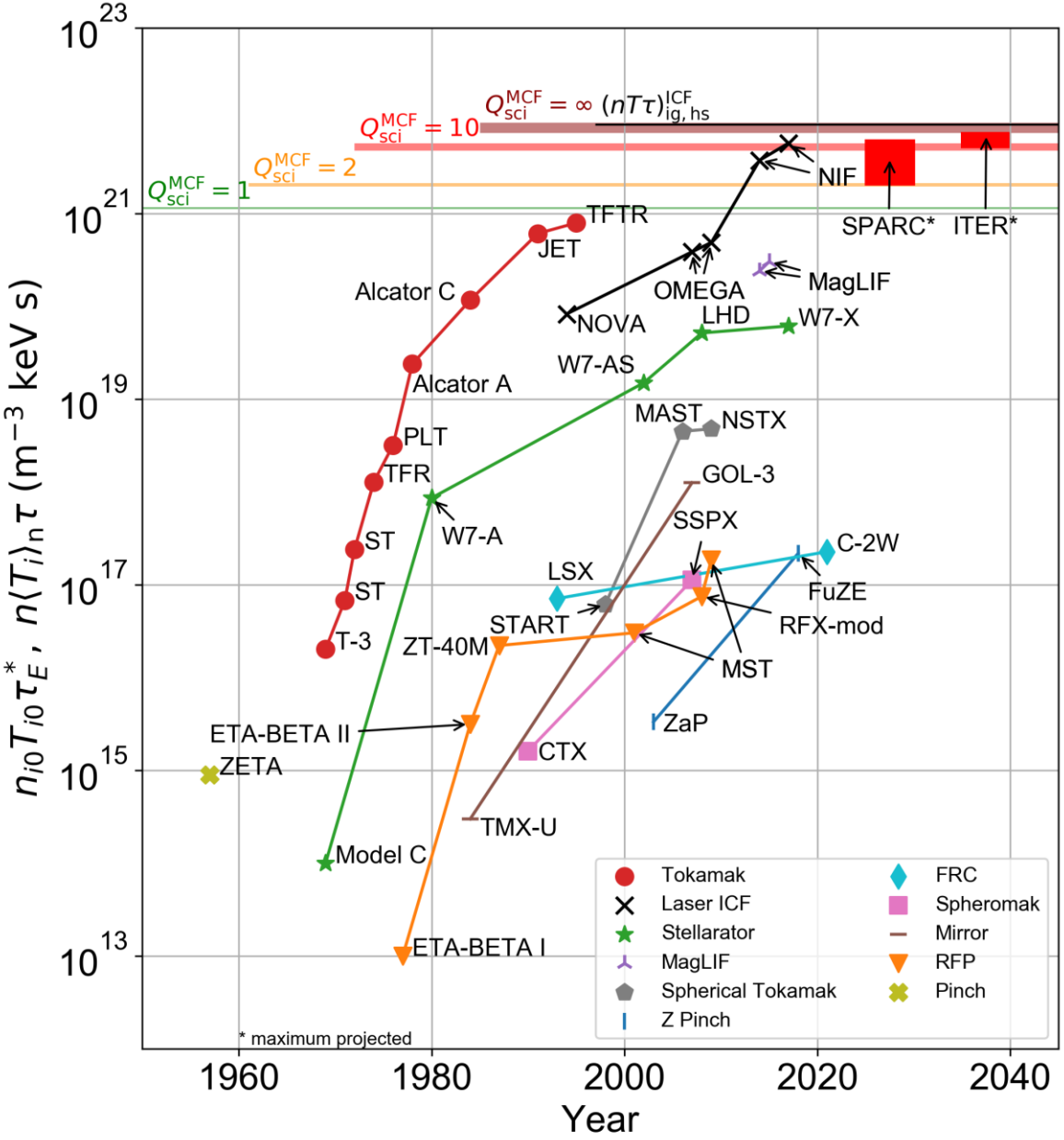

SE Wurzel, S.C. Hsu, Phys. Plasmas 29 (2022) 062103

Recent achievements of fusion community (I)

21 Dec 2021 JET (Joint European Torus, at Culham Centre for Fusion Energy in Oxfordshire, UK) **has set a world record for the most energy produced in a single fusion shot.** Pulse #99971 achieved total fusion energy of 59 MJ—more than doubling the 1997 record. It maintained an even 10 MW of fusion power, also doubling the previous record, for 5 s.

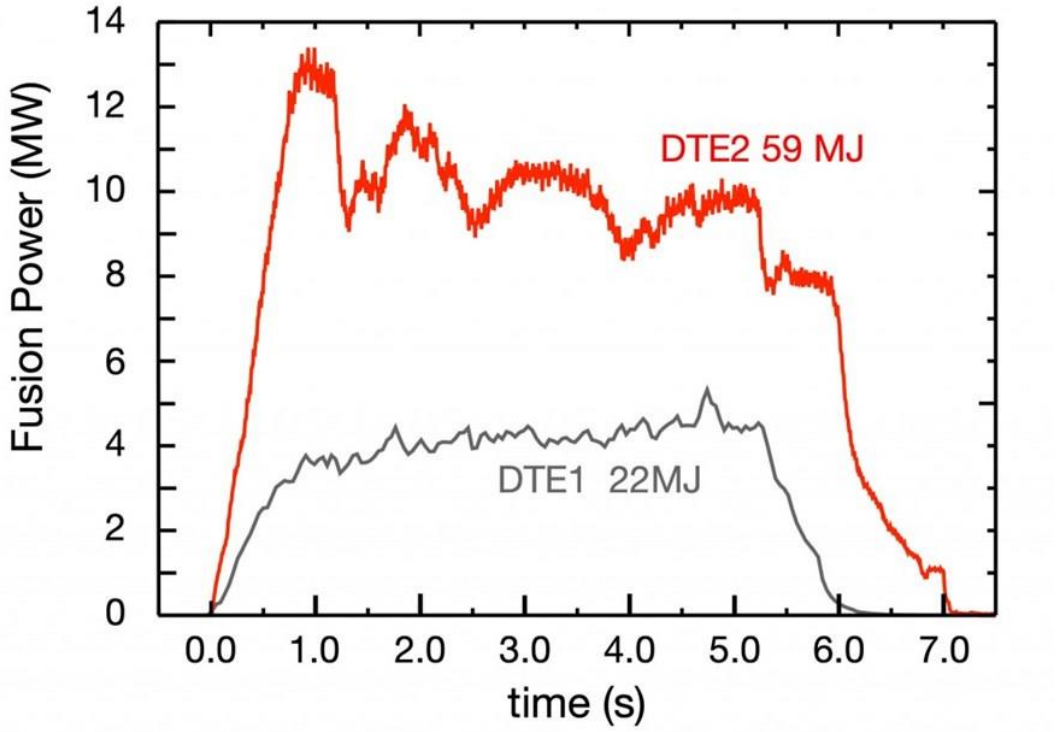

https://www.iter.org/newsline/3722#:~:text=The%20record%20shot%20was%20performed,previous%20record%2C%20for%205%20seconds.

Recent achievements of fusion community (II)

5 Dec 2022 NIF (National Ignition Facility at the Lawrence Livermore National Laboratory, Livermore, CA, USA) **A historic inertial confinement fusion experiment that applied 2.05 MJ of laser energy (192 laser beams) to compress a capsule of deuterium–tritium fuel, achieved ignition and produced 3.15 MJ of fusion energy (Q > 1)**

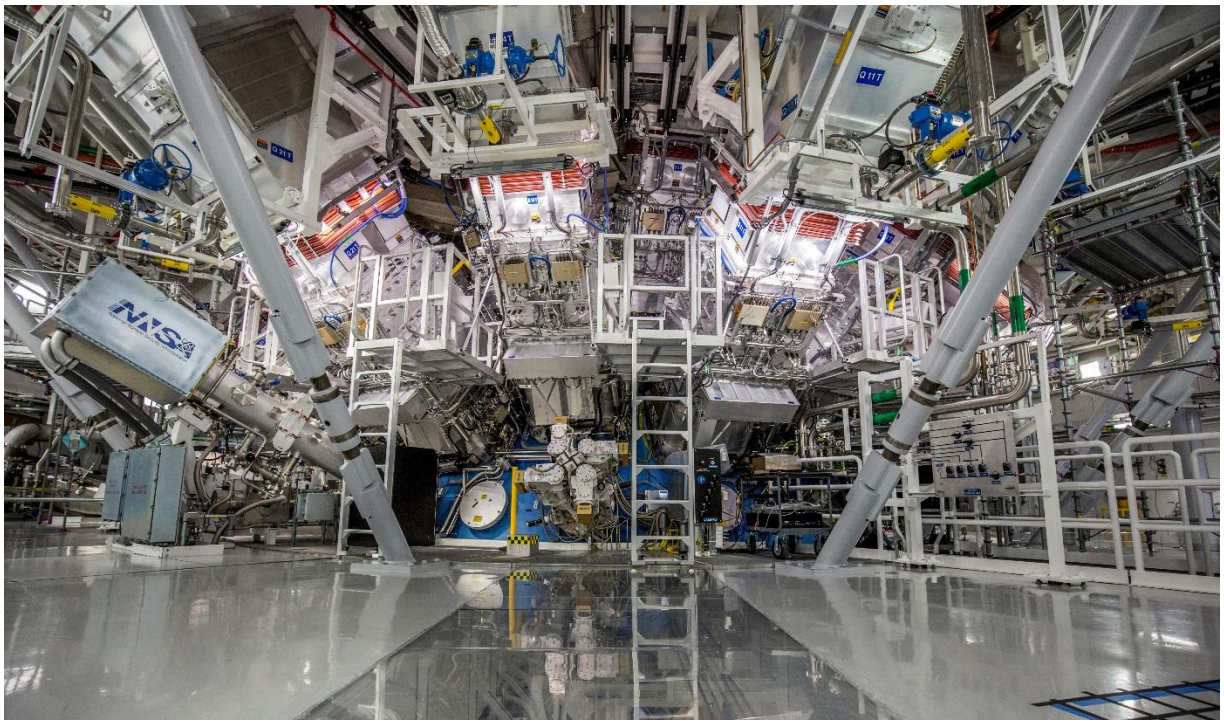

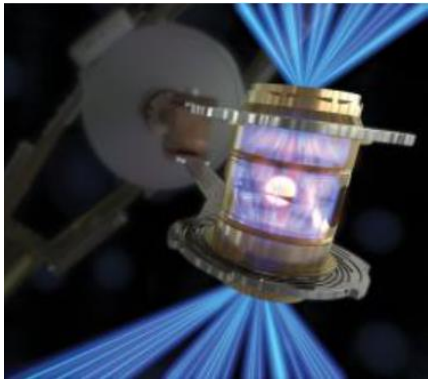

https://annual.llnl.gov/fy-2022/national-ignition-facility-2022
https://www.llnl.gov/archive/news/lawrence-livermore-national-laboratory-achieves-fusion-ignition

Benefits of fusion energy

- Clean. Zero greenhouse gases emissions. Fuel sourcing has negligible environmental impact.
- Energy security. Fuel can be sourced wherever there is water.
- Abundant. No fuel constraints or supply chain challenges.
- Safer than fission. Meltdown not possible. Operation does not require transportation of radioactive materials. Limited amount of radioactive waste, particularly those requiring long-term storage.

Magnetic confinement of plasma

Tokamak

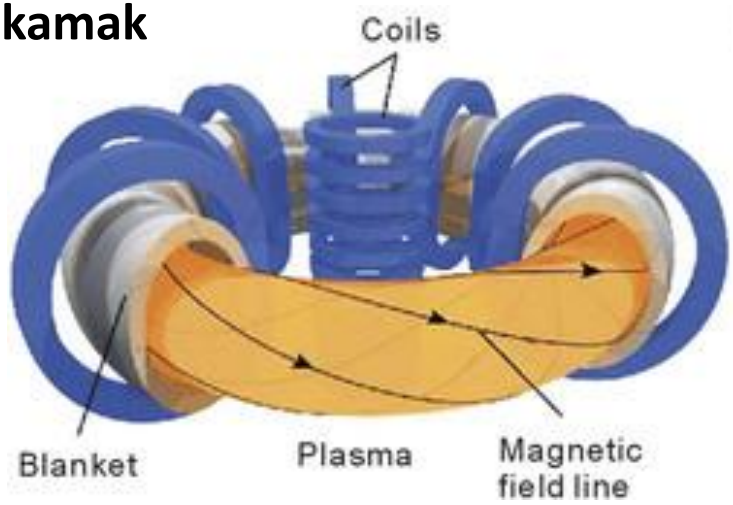

Stellarator

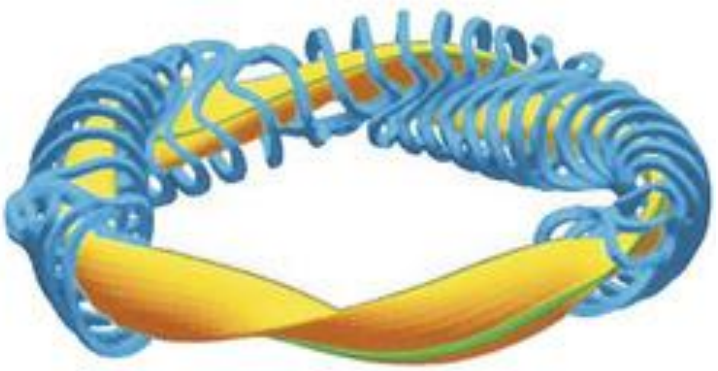

[1]

World's largest operating stellarators:

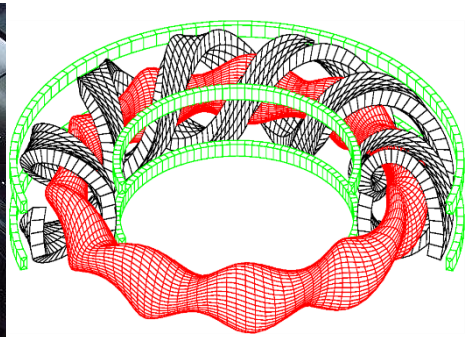

Large Helical Device (LHD) Japan [2]

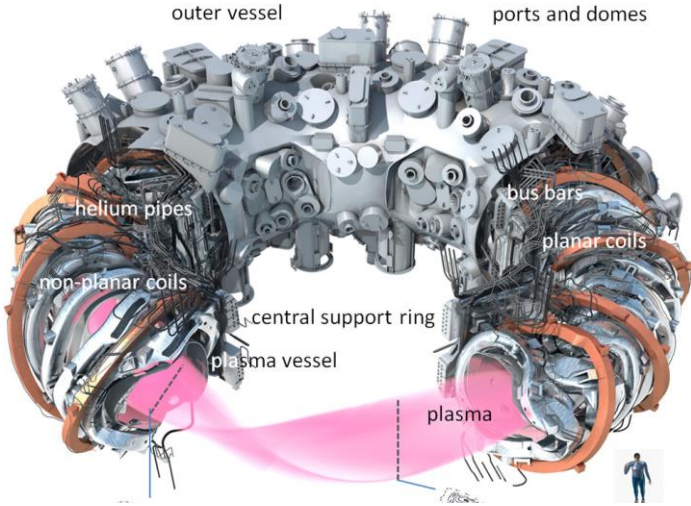

Wendelstein 7-X (W 7-X) Germany [3]

[1] Y. Xu, Matter Radiat. Extremes 1 (2016) 192-200.
[2] Justin Ruckman from Charlotte, NC, USA, CC BY 2.0 <https://creativecommons.org/licenses/by/2.0>
[3] T. Klinger, et al., Plasma Phys. Control. Fusion 59 (2017) 014018 (8pp)

Main componentts of the tokamak magnet system

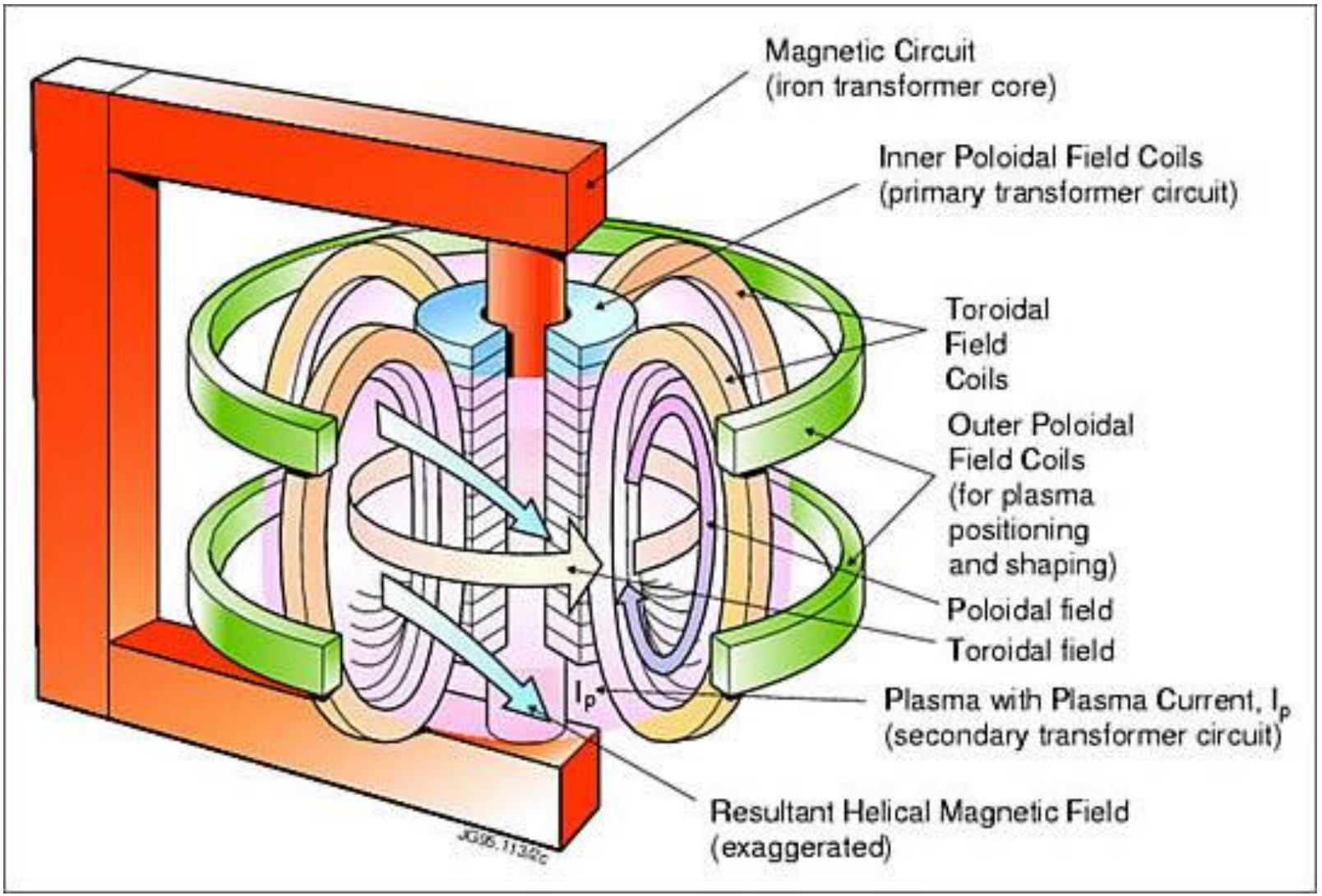

ITER– experimental reactor Cadarache (France)

Plan: 2026 r. first plasma, 2035 r. reaching Q = 10 in DT experiments (???)

- Achieve a deuterium-tritium plasma in which the fusion conditions are sustained mostly by internal fusion heating
- Generate 500 MW of fusion power from 50 MW of input heating power
- Contribute to the demonstration of the integrated operation of technologies for a fusion
- Test tritium breeding technologies
- Demonstrate the safety characteristics of a fusion device

EU – DEMO and its magnet system

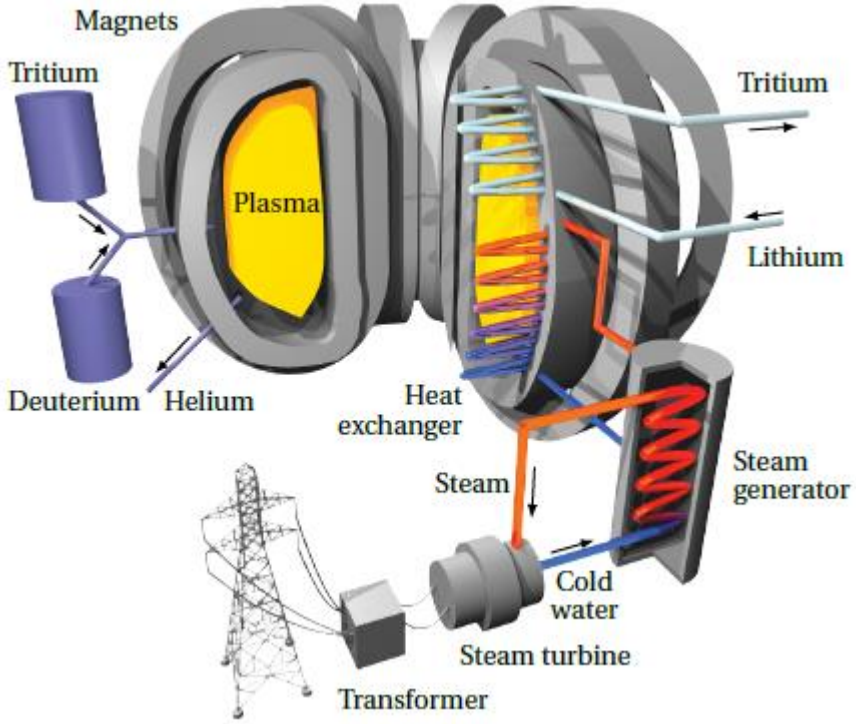

EU - DEMO – European DEMOnstration fusion power plant based on the tokamak concept with fully superconducting magnet system [4]

- Step between ITER and a commercial power plant
- Net electricity production of a few hundreds MW
- Achievement of tritium self-sufficiency
- Attaining proper availability (up to several full-power years)
- Minimization of radioactive wastes
- DEMO construction should start in the early 2030s to achieve fusion electricity by 2060

View of the DEMO coils: CS, PF and TF [5].

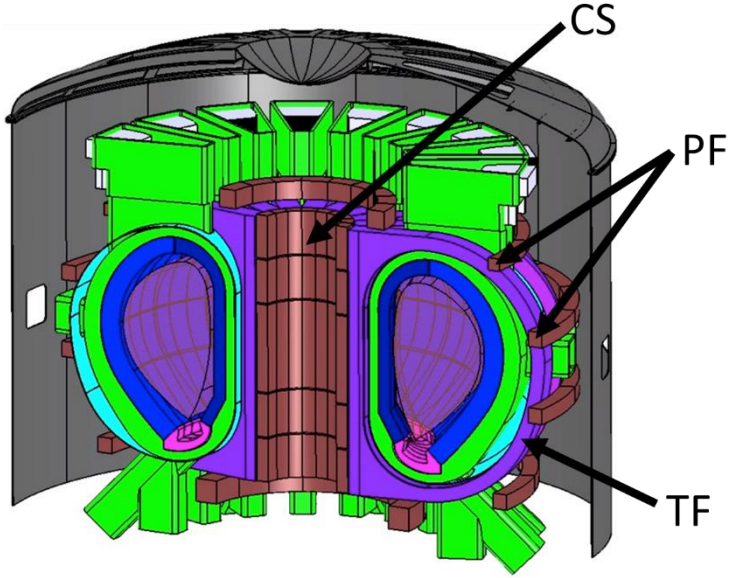

[4] ITER and fusion energy, http://iter.rma.ac.be/
[5] B. Meszaros, H. Hurzlmeier, *EU DEMO1 2015 - DEMO_TOKAMAK_COMPLEX*

Critical surface

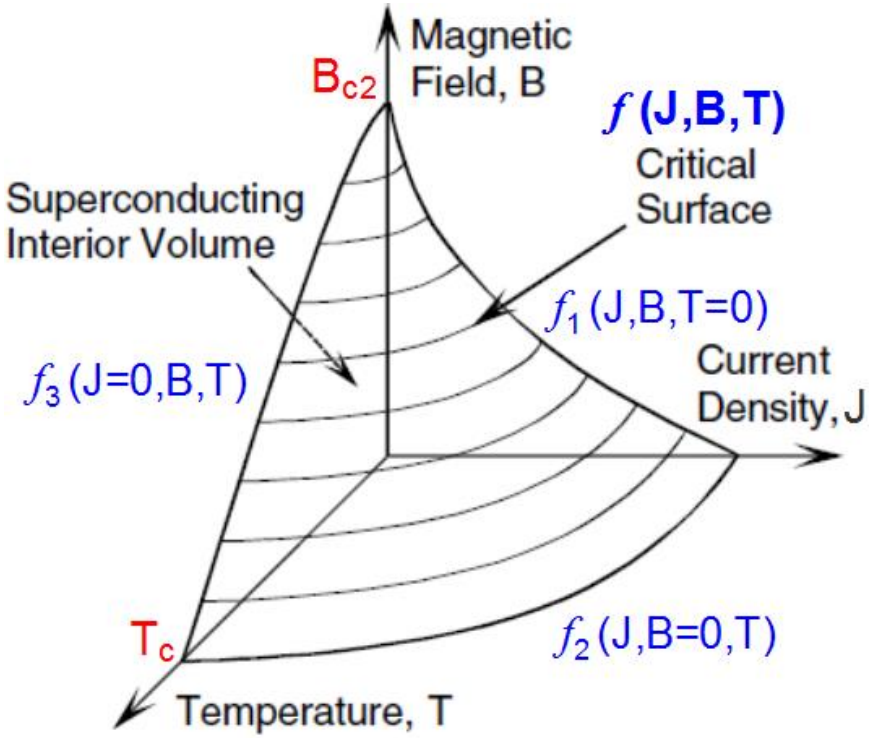

- **critical surface** is the boundary between superconductivity and normal resistivity in (J, B,T) space
- superconductivity occurs everywhere below the surface, resistance everywhere above it
- upper critical field B_{c2} (at zero temperature and current)
- critical temperature T_c (at zero field and current)
- B_{c2} and T_c are characteristic of the alloy composition, critical current density J_c depends on processing

- superconductivity exists within the phase volume bounded by the surfaces bordered by the functions : f_1 (J,B,T=0), f_2 (J,B=0,T) and f_3 (J=0,B,T)
- At the early stage of the development of a superconductor f_2 (J,B=0,T) and f_3 (J=0,B,T) are measured. For engineering purposes more useful is a general function f (J,B,T), which can also be expressed in terms of **J_c (B,T)**.
- In practice operating temperture of superconducting devices is well below T_c. Typical operating temperature is ~ 4.2 K

Critical parameters of NbTi, Nb_3Sn and REBCO

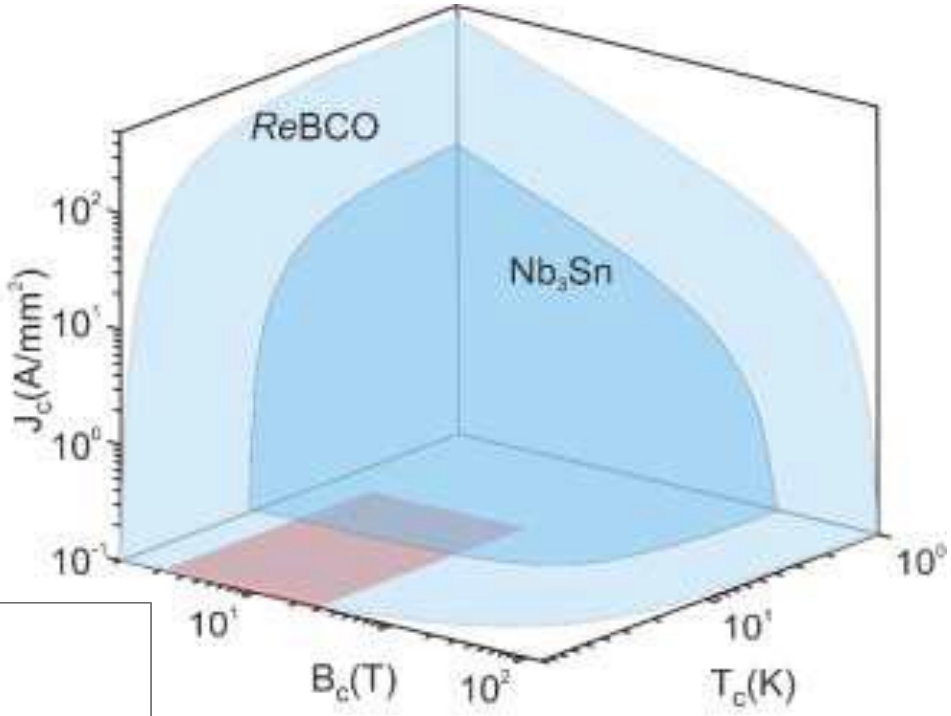

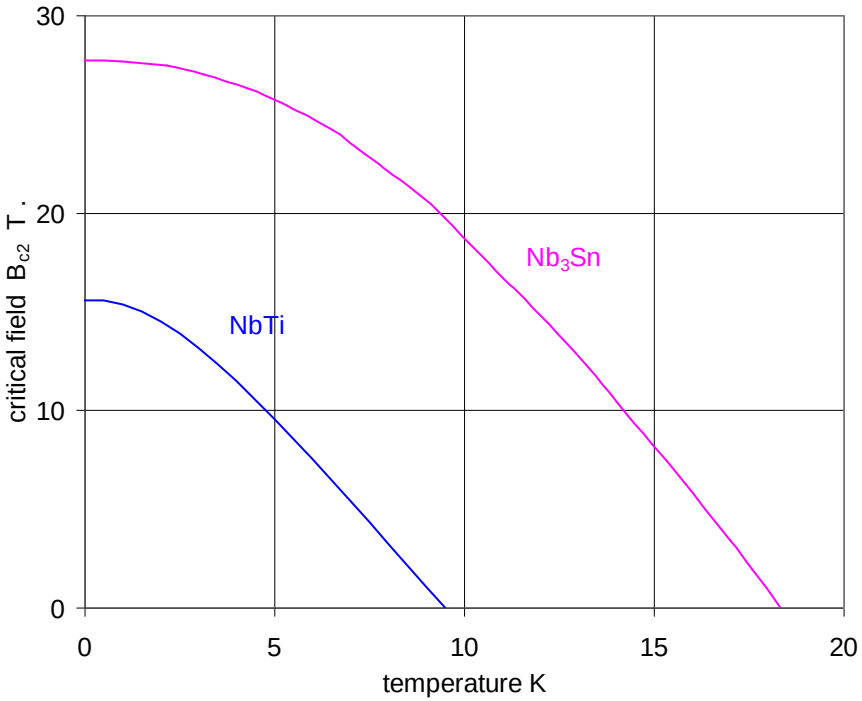

Cryogenic stabilization [6]

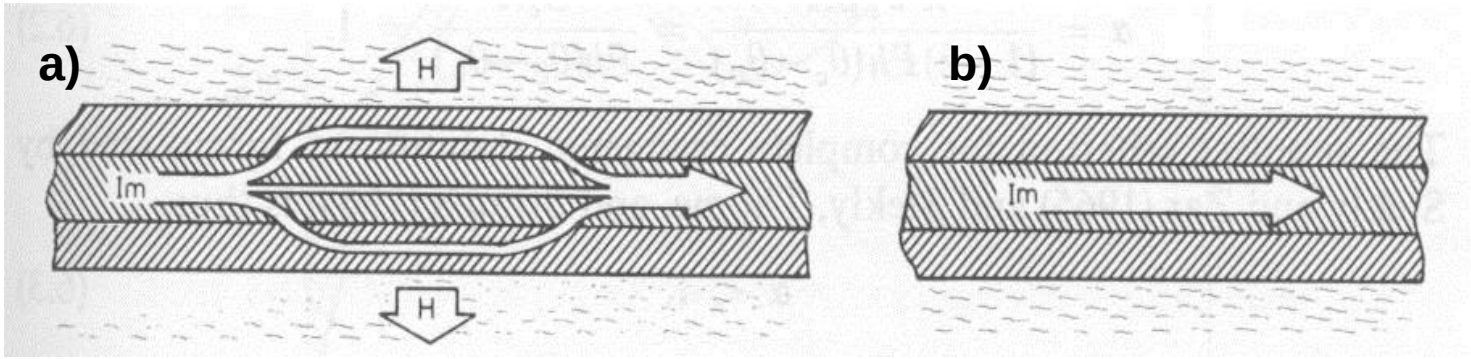

a) Following a disturbance current shares between copper and superconductor,

b) If the available cooling exceeds Joule heat generation, temperature falls below the **current sharing temperature** and current returns to the superconductor, otherwise normal zone grows => **quench**

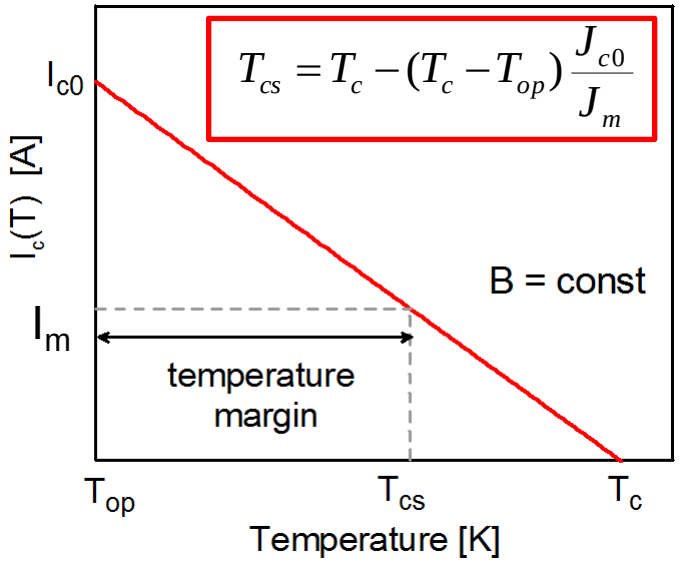

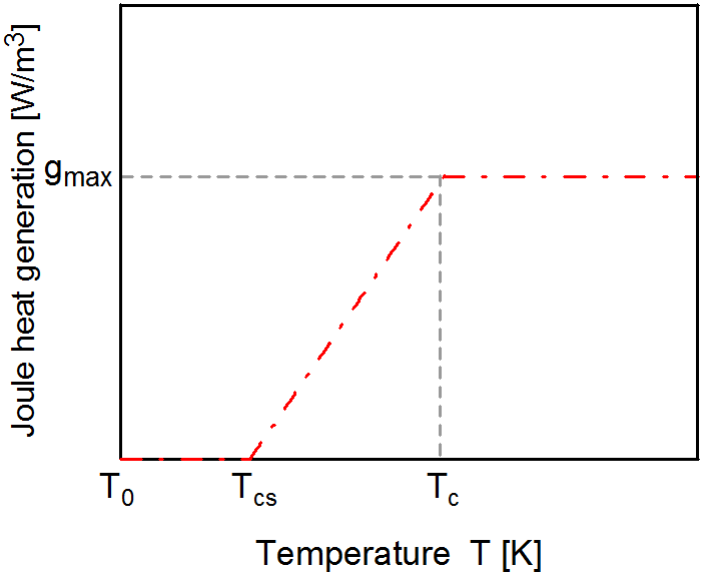

$$g_{\max} = \frac{\lambda_{sc}^2}{1-\lambda_{sc}} J_m^2 \rho_{Cu}$$

[6] *M. Wilson, Superconducting Magnets. Clarendon Press, 2002*

Force flow cooling with supercritical helium - cables

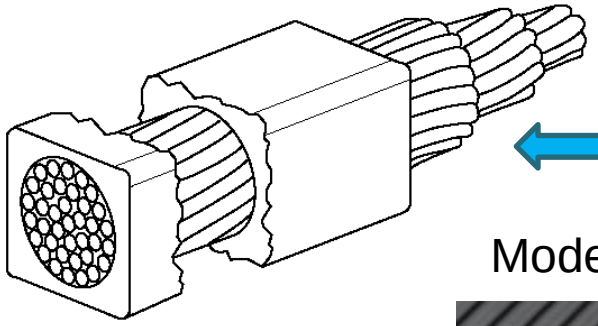

Early proposal of a **Cable-in-Conduit Conductor (CICC)** [7]

Modern realizations of CICCs

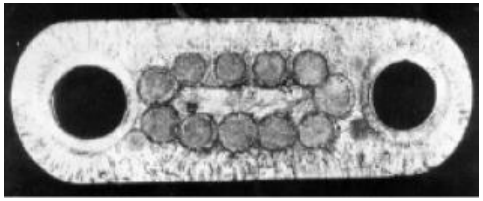

T-15, 1975-80, 5.6 kA

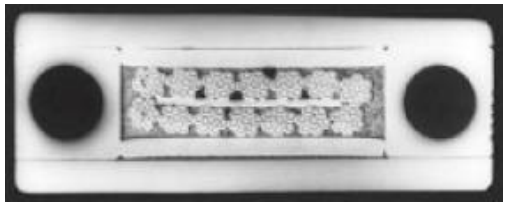

SULTAN, 1988-90, 13 kA

DPC-EX,1985-88, 10(18) kA

[7] *M.0. Hoenig, Y. Iwasa, D.B. Montgomery, A. Bejan, "Cryostabilized Single-phase Helium Cooled Bundled Conductors for Large High Field Superconducting Magnets," 6th Symposium on Engineering Problems of Fusion Research, San Diego, CA,18-21 Nov.1975, p. 586.*

EU-DEMO TF coil designs

3 LTS designs:

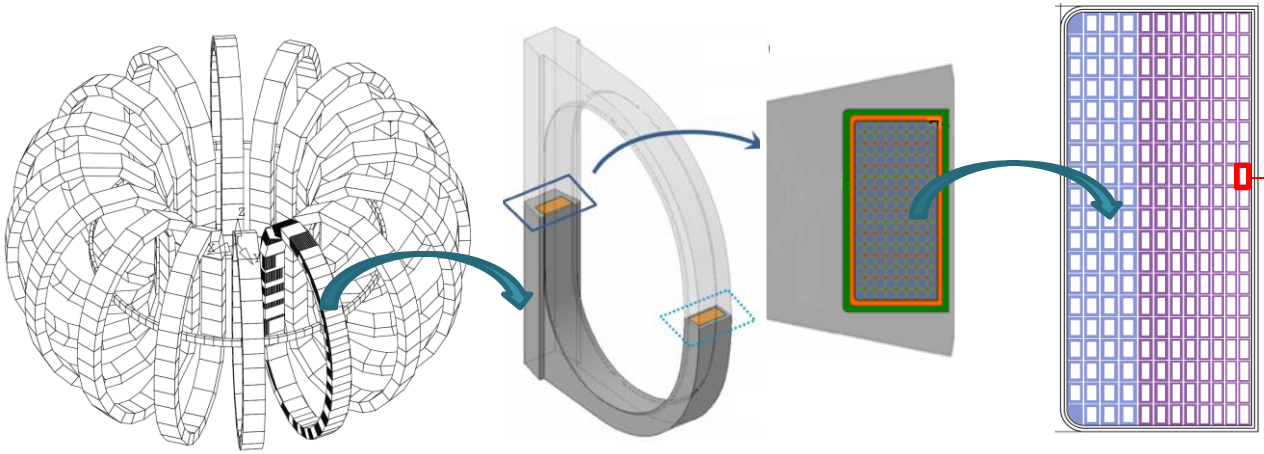

WP#1 - SPC

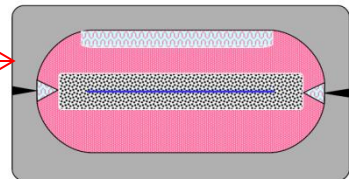

WP#2 - ENEA

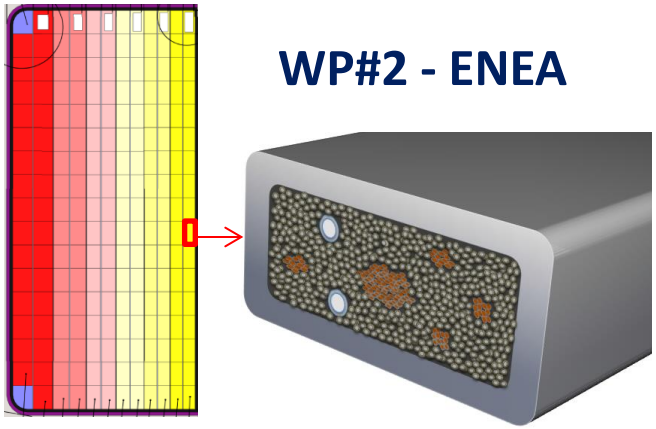

WP#3 - CEA

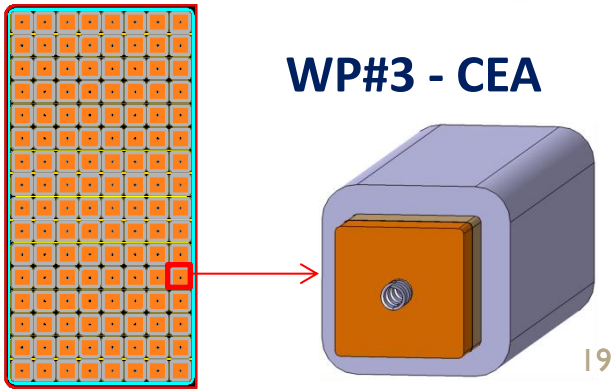

1 HTS design - KIT

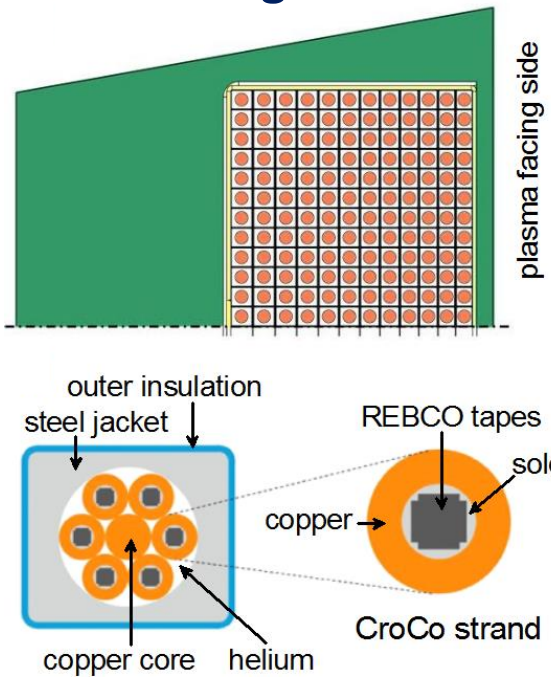

Common winding schemes

a)

b)

c)

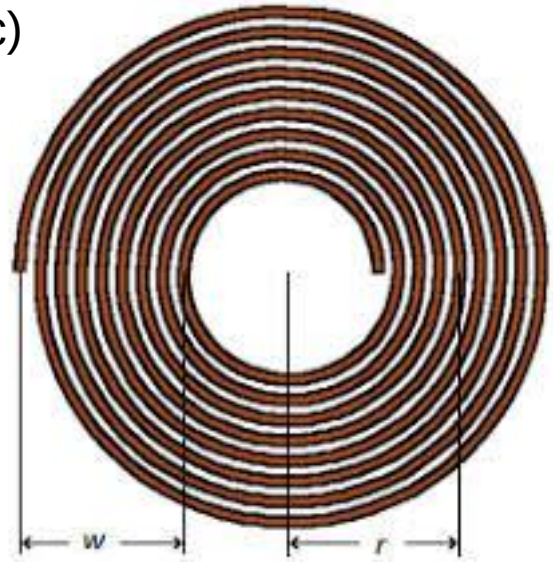

a) layer *one-in-hand* winding
b) layer *two-in-hand* winding
c) pancake winding

EU-DEMO CS coil designs

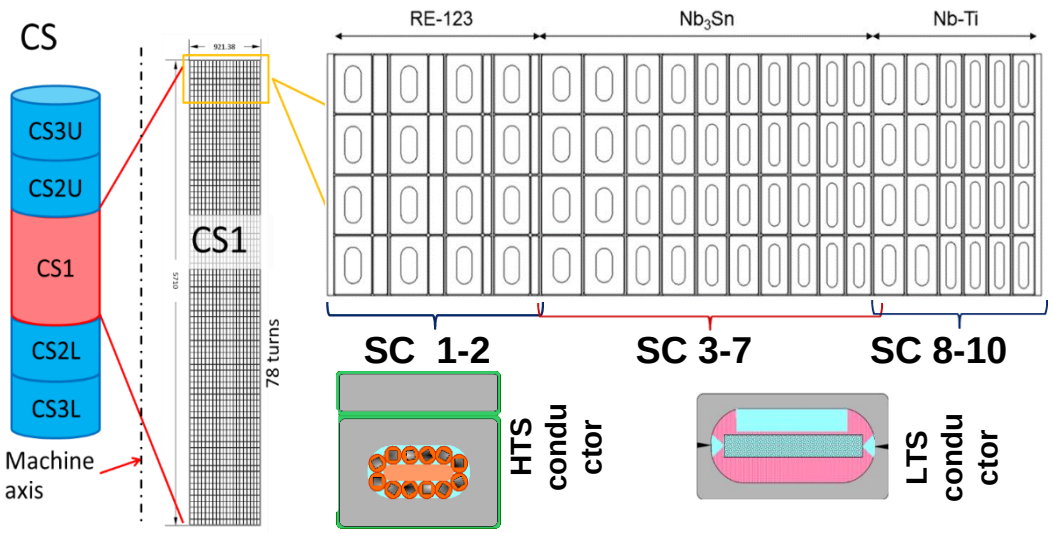

Scheme of the DEMO CS1 WP proposed by SPC

EPFL-SPC (PSI Villigen, Switzerland) proposed the design which includes 10 sub-coils (SC), each consisting of 2 layers wound with cables of the same kind. The two most inner SC, use RE-123 High T_c Superconductor (HTS), the next five SC are made of React and Wind (R&W) Nb_3Sn conductors, and the three most outer SC utilize NbTi.

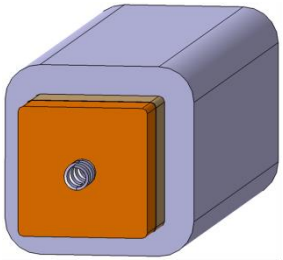

CEA conductor design

According to the CEA (Cadarache, France) design, the CS1 module will be double pancake wound using a square wind & react Nb_3Sn CICC, with a central cooling channel delimited from the bundle region with a steel spiral.

EU-EMO PF coils – CEA design

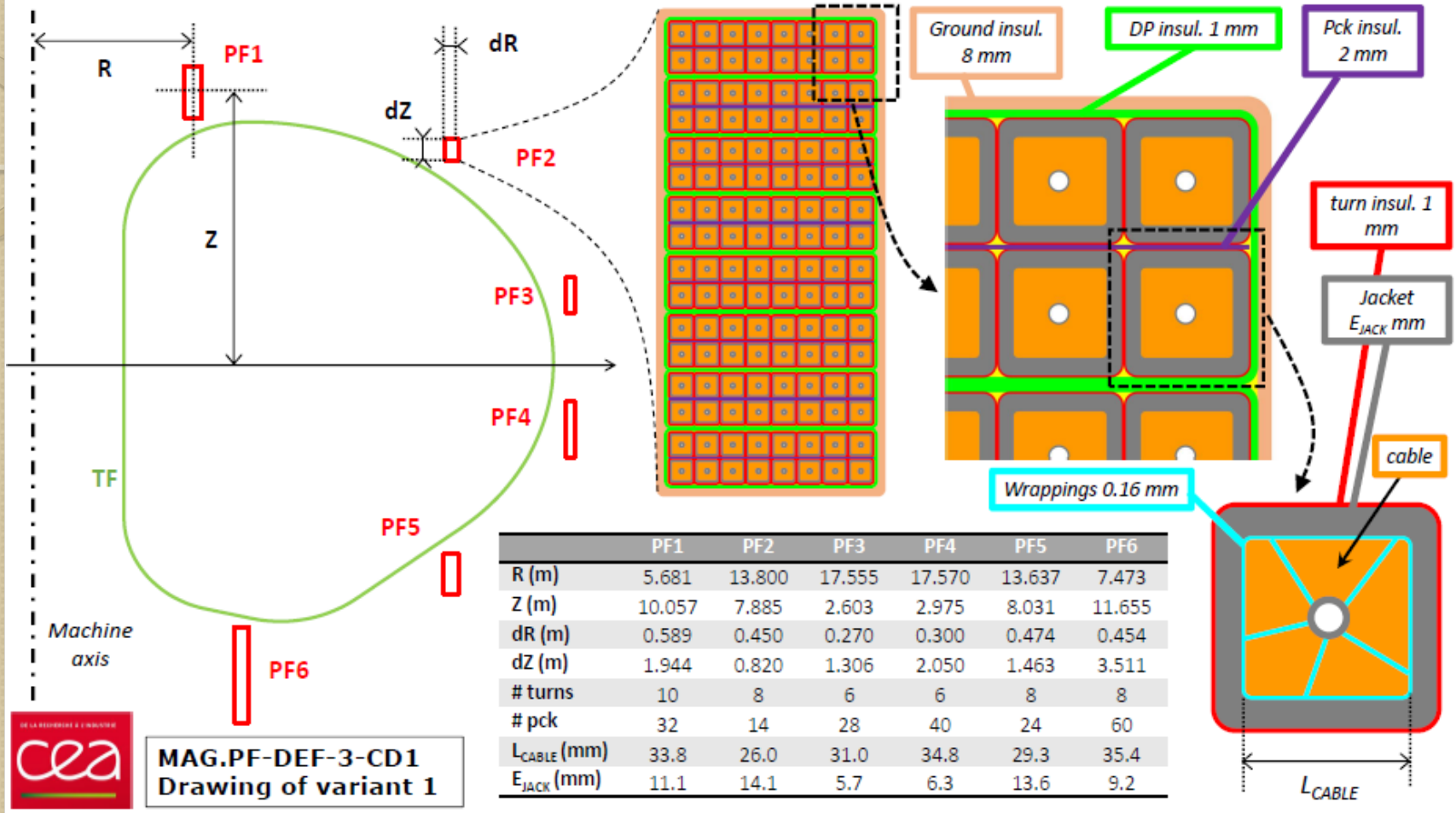

	PF1	PF2	PF3	PF4	PF5	PF6
R (m)	5.681	13.800	17.555	17.570	13.637	7.473
Z (m)	10.057	7.885	2.603	2.975	8.031	11.655
dR (m)	0.589	0.450	0.270	0.300	0.474	0.454
dZ (m)	1.944	0.820	1.306	2.050	1.463	3.511
# turns	10	8	6	6	8	8
# pck	32	14	28	40	24	60
L_{CABLE} (mm)	33.8	26.0	31.0	34.8	29.3	35.4
E_{JACK} (mm)	11.1	14.1	5.7	6.3	13.6	9.2

Main features of the DEMO PF coils design proposed by CEA [6]

Each of 6 PF coils is double pancake (DP) wound using a different square NbTi Cable-in-Conduit conductor [6].

[6] L. Zani. *CEA PF winding pack design*, Final report for the task MAG-2.1-T026-D002 (2020), https://idm.euro-fusion.org/?uid=2N9WUY

Analyses of superconducting coils designs

All candidate coil design are subjected to comprehensive analyses:

- electromagnetic
- mechanical
- thermal - hydraulic

in order to verify if the proposed coil designs fulfill the acceptance criteria and to provide the information for further optimization of the conductors' dimensions and layouts

Thermal-hydraulic analyses of superconducting cables designed for EU-DEMO

- Estimation of the maximum He mass flow rate in a coil (useful information designers of the DEMO cryogenics system)
- Verification if the minimum temperature margin in all conductors at operating conditions is sufficiently large:

$$\textbf{minimum } \Delta T_{marg} > 1.5 \text{ K} \quad [7]$$

$$\text{where } \Delta T_{marg}(x,t) = T_{cs}(x,t) - T_{sc}(x,t)$$

- Verification if the maximum temperature during quench is sufficiently low:

$$\textbf{max } T_{jacket} < 150 \text{ K} \quad [7]$$

$$\textbf{max } T_{strands} < 250 \text{ K}$$

[7] V. Corato et al., *Progress in the design of the superconducting magnets for the EU DEMO*, Fus. Eng. Des. 136 (2018) 1597–1604

Tools (I)

- Simplified models [7]
  - Hydraulic analysis (at no heat loads)

T_{in} = 4.5 K, p_{in} = 6 bar, Δp = 1 bar – assumed cooling conditions (ITER like)

$$h(T_{in}, p_{in}) = h(T_{out}, p_{out}) \Rightarrow T_{out} = 4.602 \text{ K}$$

$$\frac{\Delta p}{L} = \frac{2\dot{m}^2 f}{D_h \rho A_{He}^2} \Rightarrow \dot{m}_{max}$$

  - Steady state heat removal model (SM) [7,8]

$$\begin{cases} \dot{m}_1 \dfrac{dh_1}{dx} + c\dot{m}_2 \dfrac{dh_2}{dx} = \dot{Q}_L(x) \\ \dfrac{dp_i}{dx} = -\dfrac{2\dot{m}_i^2 f_i(\mathrm{Re}_i)}{D_h \rho(T, p_i) A_{He}^2} + v_i^2 \dfrac{d\rho_i}{dx} \end{cases}$$

$\dot{Q}_L$ – assumed heat loads (W/m)

c – numer of cooling channels

$$\begin{cases} T(0) = T_{in} \\ p_i(0) = p_{in} \end{cases}$$ boundary conditions

$$\frac{dh_i}{dx} = C_p(T, p_i)\frac{dT}{dx} + \frac{1}{\rho(T, p_i)}\left[1 - \alpha(T, p_i)\cdot T\right]\frac{dp_i}{dx} \Rightarrow T(x), p_i(x), m_i$$

$$J_C(B(x), T_{cs}(x)) = J_{op} \Rightarrow T_{cs}(x) \Rightarrow \Delta T_{marg}(x)$$

Tools (II)

- THEA code [9]

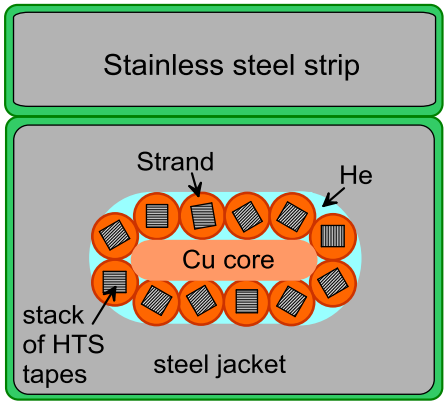

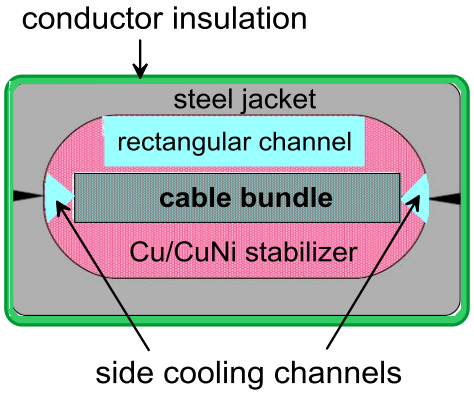

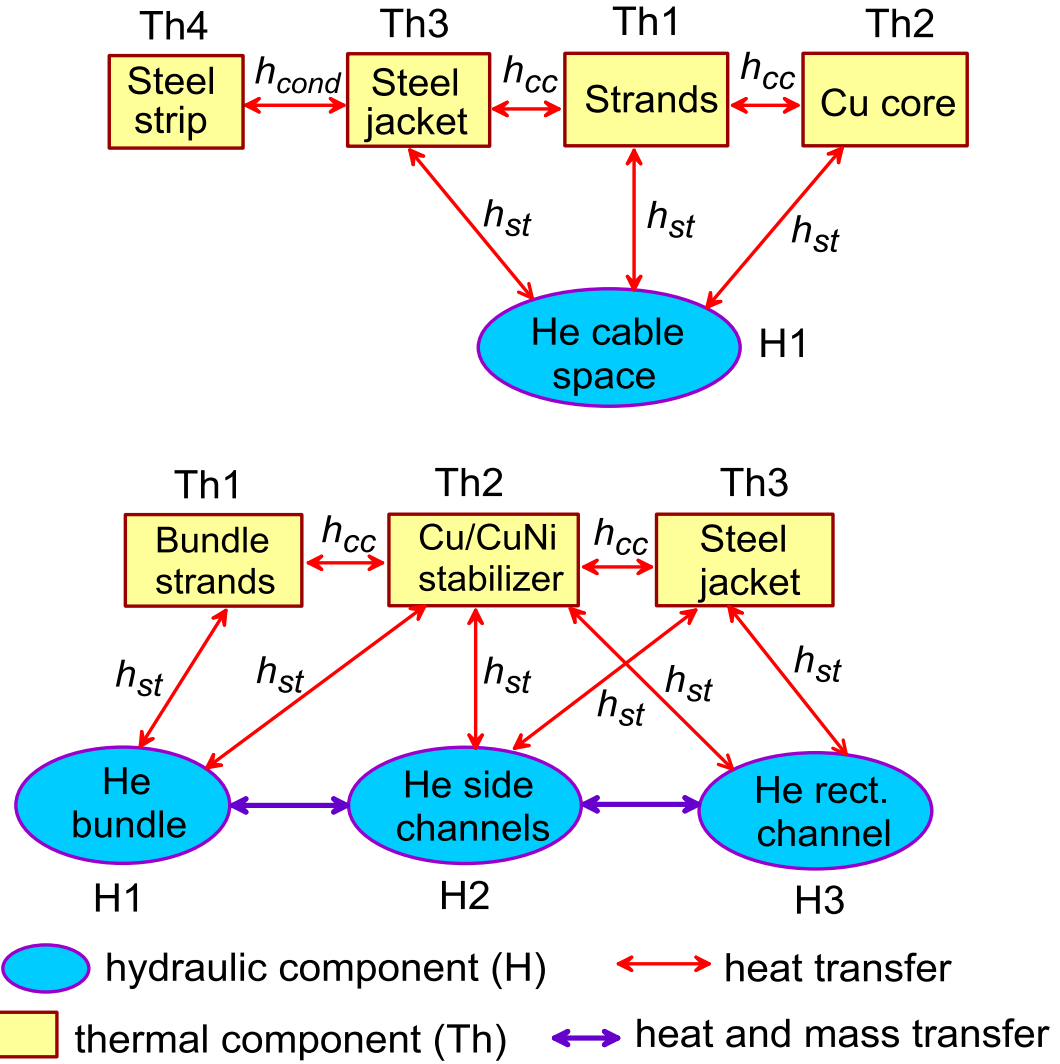

[7] M. Lewandowska, K. Sedlak, Thermal-hydraulic analysis of LTS cables for the DEMO TF Coil, IEEE Trans. Appl. Supercond. 24 (2014), 4200305.

[8] M. Lewandowska, A. Dembkowska, K. Sedlak, Thermal-hydraulic analysis of different design concepts of the LTS TF coil winding pack for EU-DEMO, ELMECO & AoS, 2017, doi:10.1109/ELMECO.2017.8267763.

[9] THEA—Thermal, Hydraulic and Electric Analysis of Superconducting Cables. User's Guide Version 2.3, CryoSoft, 2016, https://supermagnet.sourceforge.io/manuals/Thea_2.3.pdf.

Input data

- Conductor design
  - Conductor layout
  - Materials, scaling law for the superconductor $J_c = f(B,T)$
  - Hydraulic resistance and heat transfer characteristics (correlations for the friction factor and Nusselt number for each channel of flow)
- Operating current
  - Constant current for TF coils
  - Current scenario for CS i PF coils
- Magnetic field profile along the conductor
  - Constant for TF coils
  - Time dependent for CS and PF coils
- Heat load profile along the conductor
  - Nuclear heat load for TF coils
  - Heat loads due to AC losses in CS and PF
  - Assumed heat disturbance in *quench* simulations

Current scenario – CS and PF coils

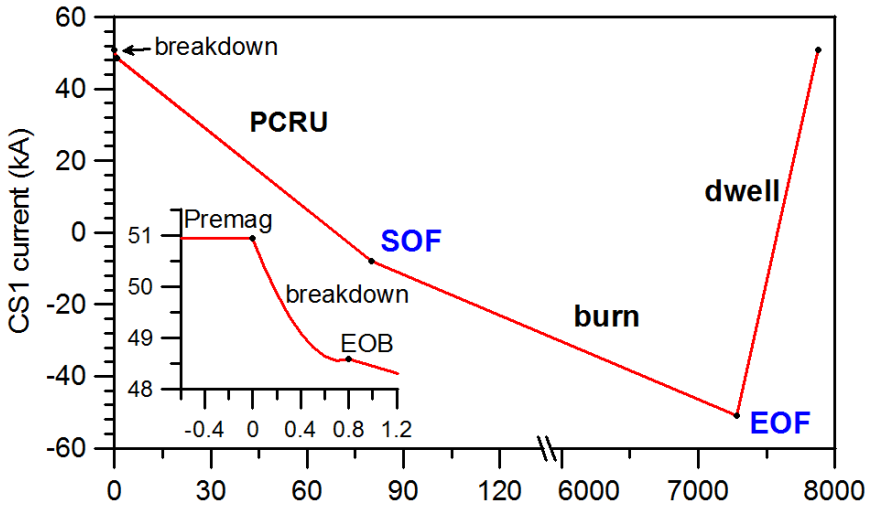

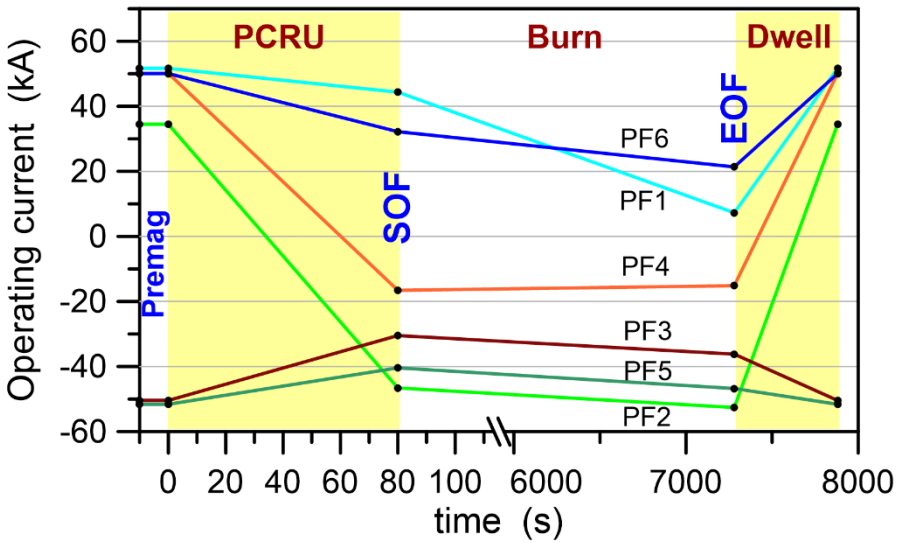

Normal operation

„4 points" simplified current scenario includes the following phases: **Premag**netization: 10 s

Plasma **C**urrent **R**amp-**U**p (**PCRU**): 80 s

Burn: 7200 s

Dwell: 600 s [10]

Actually the PCRU phase starts with the fast **breakdown** [11] lasting ~0.8 s (which is simulated separately)

[10] G. Federici, et al., *DEMO Design Activity in Europe: Progress and Updates*, Fus. Eng. Des. 136, Part A (2018) 729-741

[11] M. Matei, R. Wenninger , *DEMO AR = 3.1 Preliminary Breakdown magnetic analyses*, Annex-B to Mobility Report EFDA PMU Garching 30/7/15-13/8/15

Magnetic field maps

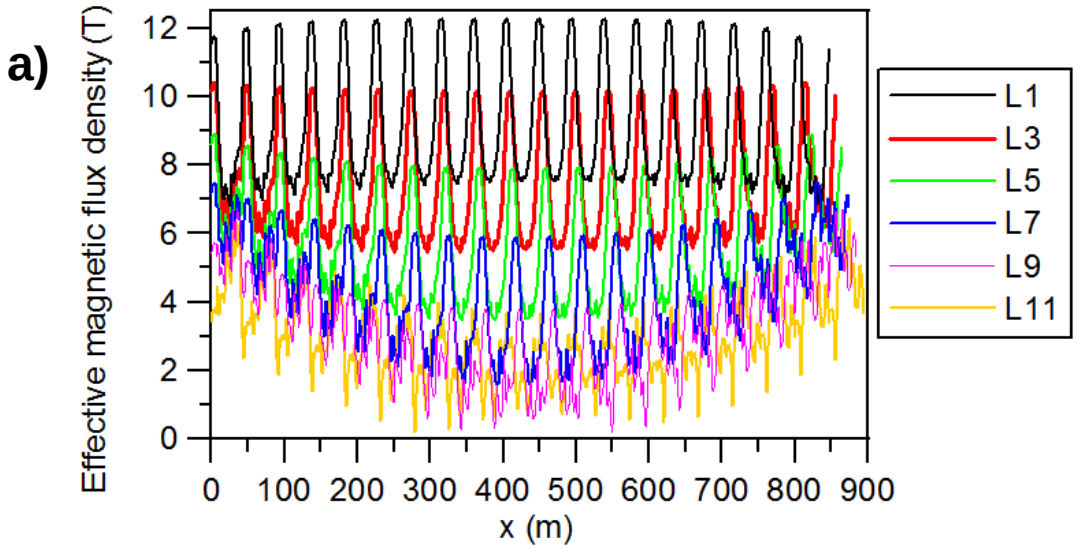

a) Layer wound TF coil (SPC design) [8]

b) Pancake wound TF coil (CEA design) [12]

c) Pancake wound CS1 coil (CEA design) [13]

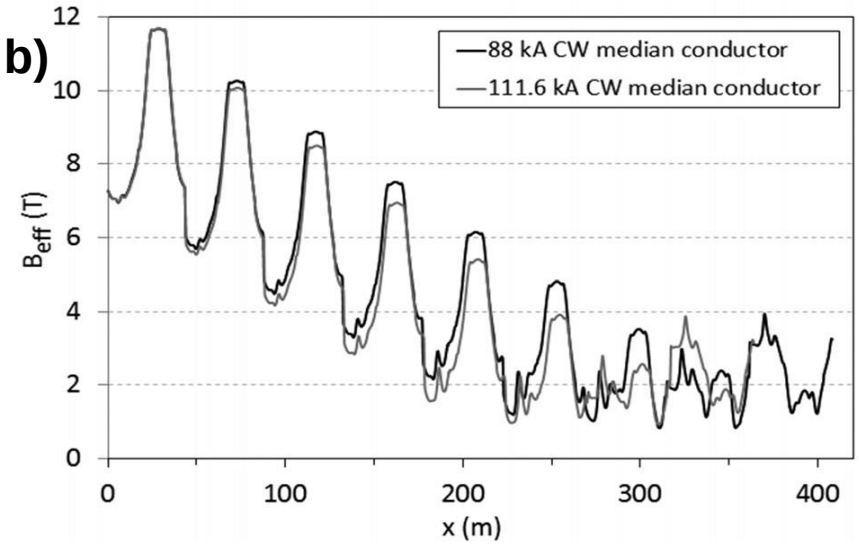

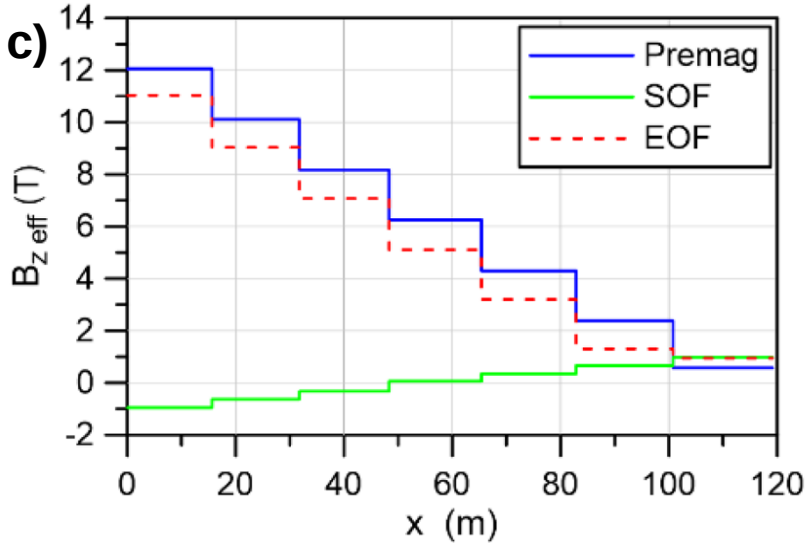

[12] R. Vallcorba, et. al., *Thermohydraulic Analyses on CEA Concept of TF and CS Coils for EU-DEMO*, IEEE Trans. Appl. Supercond. 28 (2018) 4202605.

[13] A. Dembkowska, M. Lewandowska, L. Zani, B. Lacroix, *Thermal-hydraulic analysis of the DEMO CS coil designed by CEA,* Fusion Eng. Des. 171 (2021) 112557.

Magnetic field maps

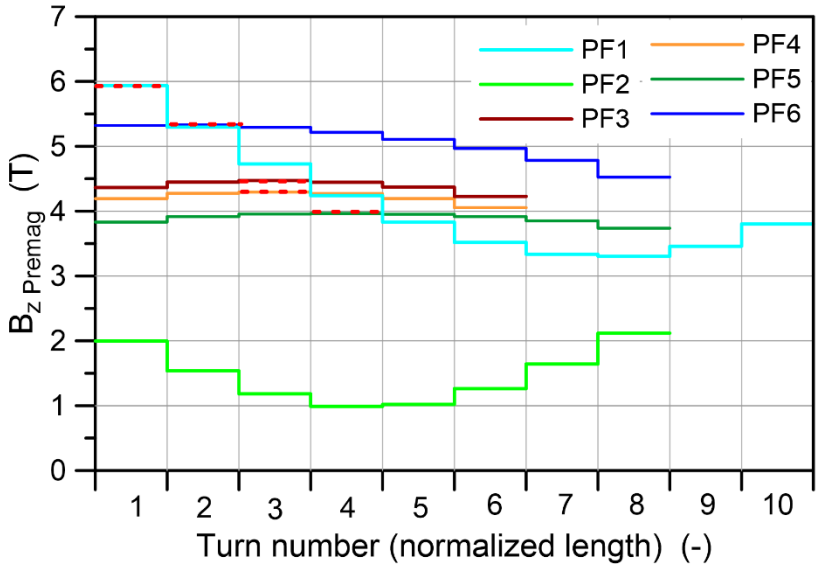

Pancake wound PF coils (CEA design) [14]

[14] M. Lewandowska, A. Dembkowska, L. Zani, B. Lacroix, *Thermal-Hydraulic Analysis of the DEMO PF Coils Designed by CEA,* submitted for publication to Cryogenics

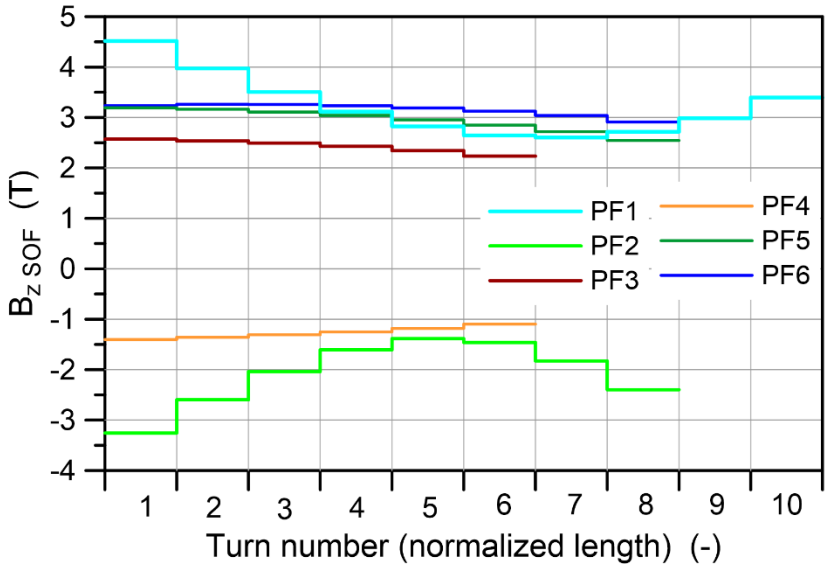

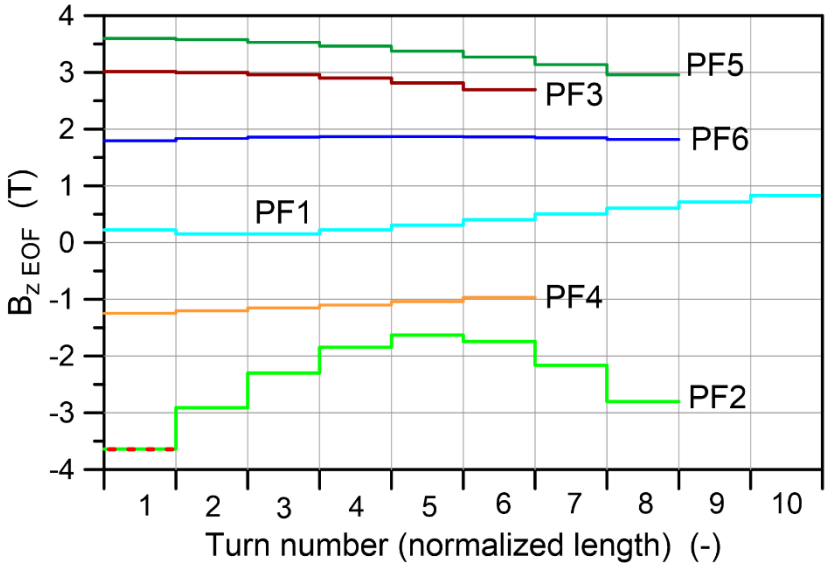

Neutronic heat loads in TF coils

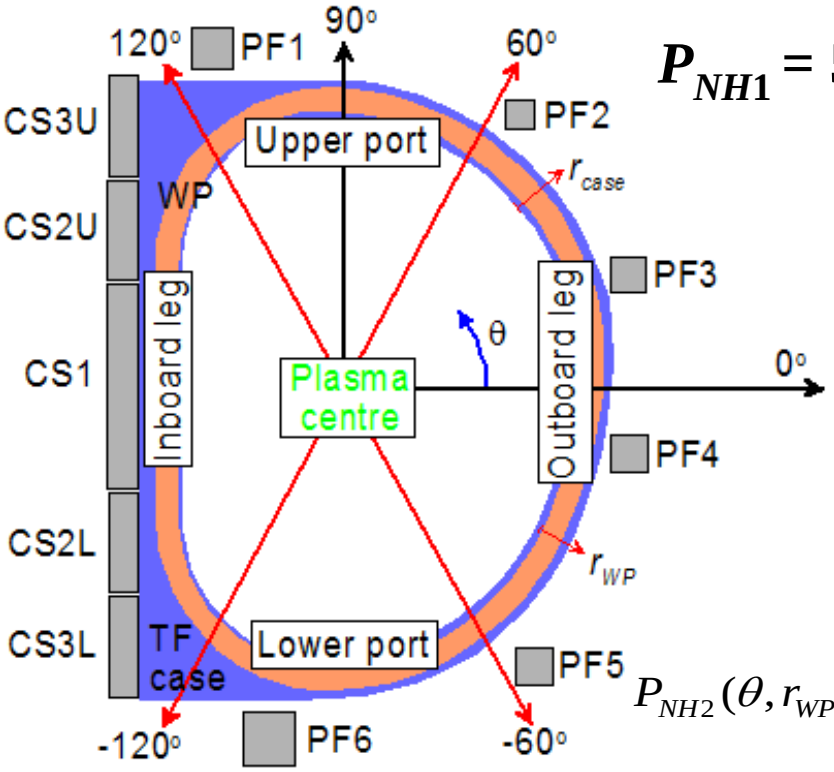

$$P_{NH1} = 50\ \mathrm{W/m^3}\cdot\exp(-r_{case}/0.140\ \mathrm{m})\ [15]\quad (1)$$

Eq. (1) served as a reference for the present WP designs and as a basic approach in our analysis. However, the most recent neutronic study, provided the new more advanced formula for NH load in the WP [10]:

$$P_{NH2}(\theta, r_{WP}, z) = \begin{cases} 2.5\ \mathrm{W/m^3} & \text{for } -60^\circ < \theta < 60^\circ \\ 50\ \mathrm{W/m^3}\cdot\exp(-r_{WP}/0.125\,\mathrm{m}) & \\ & \text{for } -120^\circ < \theta < 120^\circ \\ 20 + 16|z|\ \mathrm{W/m^3} & \text{for } 60^\circ \le \theta \le 120^\circ \\ & \text{or } -120^\circ \le \theta \le -60^\circ \end{cases}$$

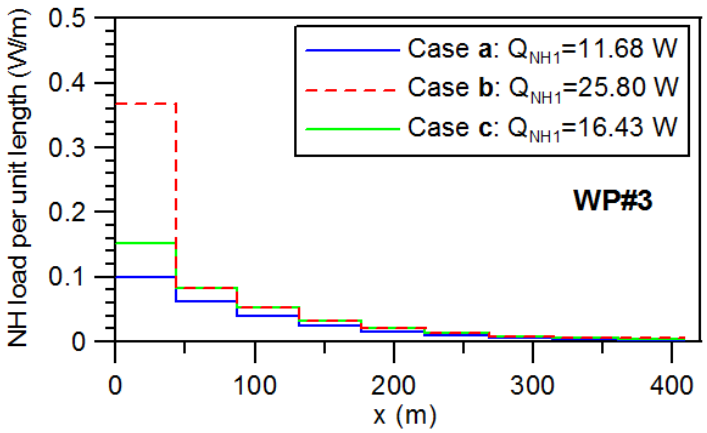

[15] L. Zani, U. Fischer, *Advanced definition of neutronic heat load density map on DEMO TF coils*, Memo for WPMAG-MCD-2.1/2.2/ 3.3, v. 1.0, 2014, https://idm.euro-fusion.org/?uid=2MFVCA

[16] M. Coleman, *Advanced definition of neutronic heat load density map on DEMO TF coils*, Memo for WPMAG-MCD-2.1/2.2/3.3, v.2.0, 2016, https://idm.euro-fusion.org/?uid=2MFVCA

Heat loads due to AC losses in CS and PF coils

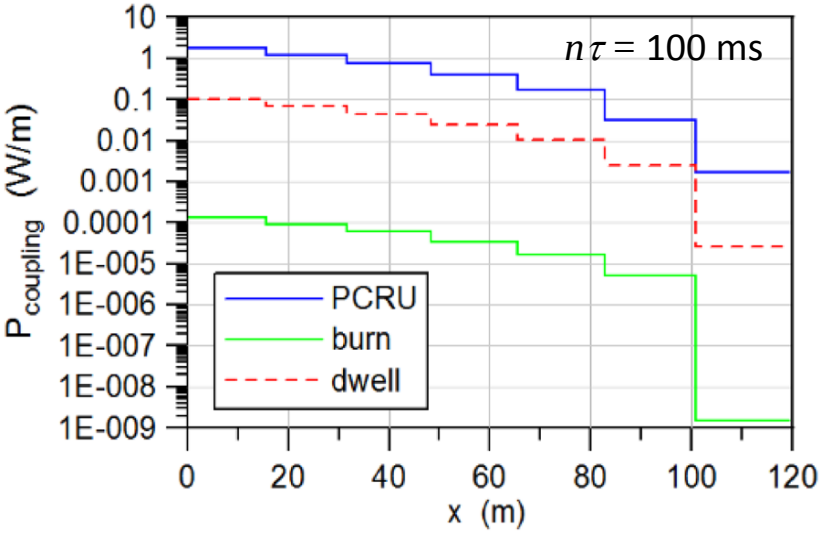

Coupling losses at normal operation of the CS1 conductor (CEA design)

- Coupling losses

$$P_{coupling}(x,t) \approx \frac{n\tau S}{\mu_0}\left[\frac{\partial B_{z\,eff}(x,t)}{\partial t}\right]^2$$

calculated using several trial values, e.g. $n\tau$ = 100, 200, 400 ms

- Hysteresis losses

$$P_{hyst}(x,t) \approx \frac{2}{3\pi} J_c(B_{z\,eff}, T) d_{eff} \left|\frac{\partial B_{z\,eff}(x,t)}{\partial t}\right|$$

where:

J_c - critical current density,

$d_{eff} \approx 5$ μm - effective filament diameter

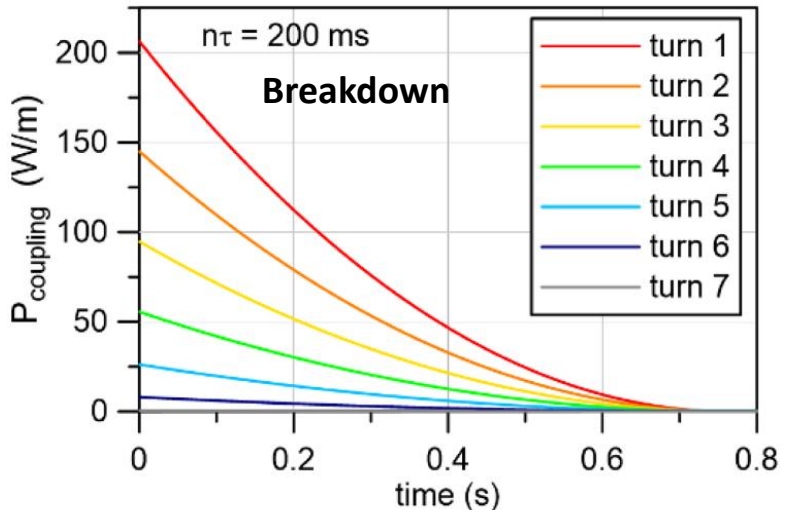

Heat loads due to AC losses (II)

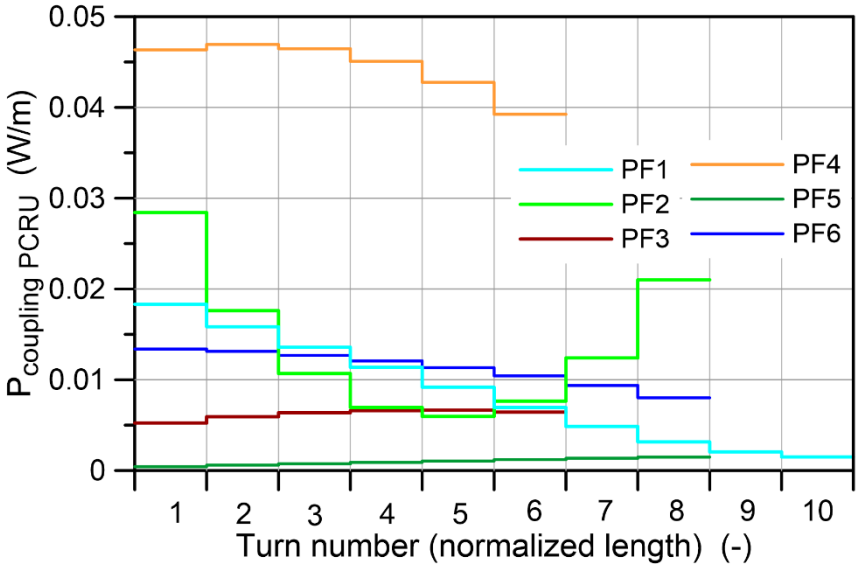

Pancake wound PF coils (CEA design) [14]

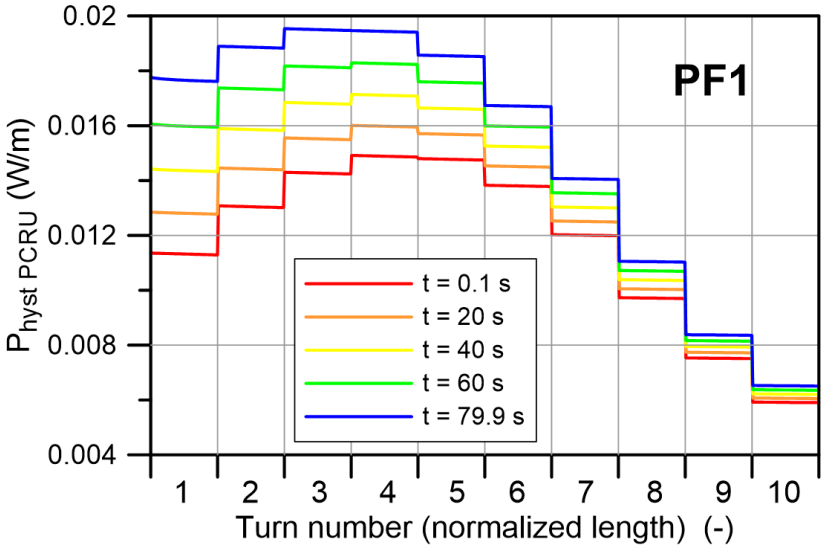

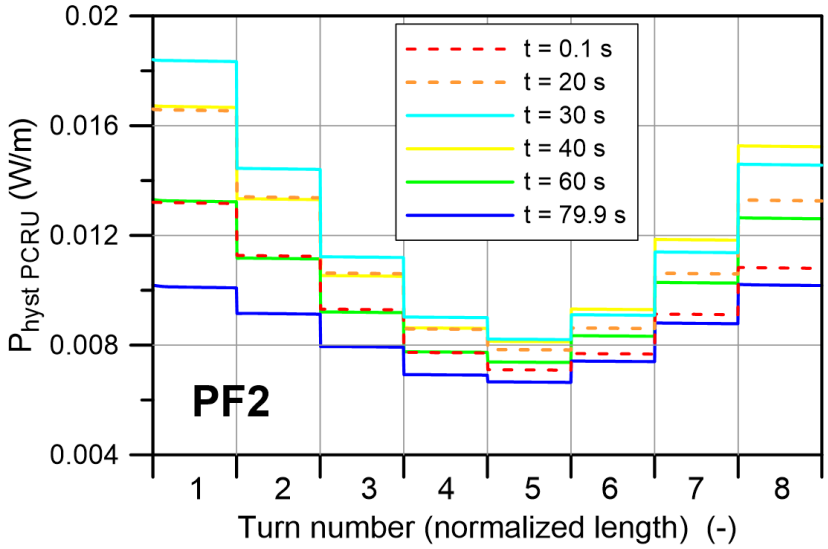

Quench simulations

- Full conductor length subjected to the expected MF is simulated using THEA [9].
- Adiabatic and fixed pressure (infinite reservoir) boundary conditions are imposed at both ends of a conductor.
- At first simulations of normal operation are performed, starting from the constant initial conditions: $T(x) = T_{in}$, $p(x) = p_{in}$ until the steady state is reached. The obtained steady state temperature, pressure and mass flow profiles, after validation against the simplified model, are used as the initial conditions for the subsequent quench simulations.
- Quench is initiated by a heat disturbance of length 10 cm and duration 100 ms imposed at the ΔT_{marg} minimum. The disturbance energy is planned to be 2 x MQE (Minimum Quench Energy, estimated by the iterative trial and error procedure).
- In quench simulation we use refined initial mesh with automatic adaptivity. In the 1 m long refined region around the disturbance location the distance between nodes was 2 cm, in the rest of a cable – 25 cm.
- The quench detection threshold is set at 0.1 V, with an additional delay of 1.1 s before the start of exponential current dump with the characteristic time constant
- Magnetic field profile varies proportionally to the operating current.

Results – temperature margin at EOF in TF coils [8]

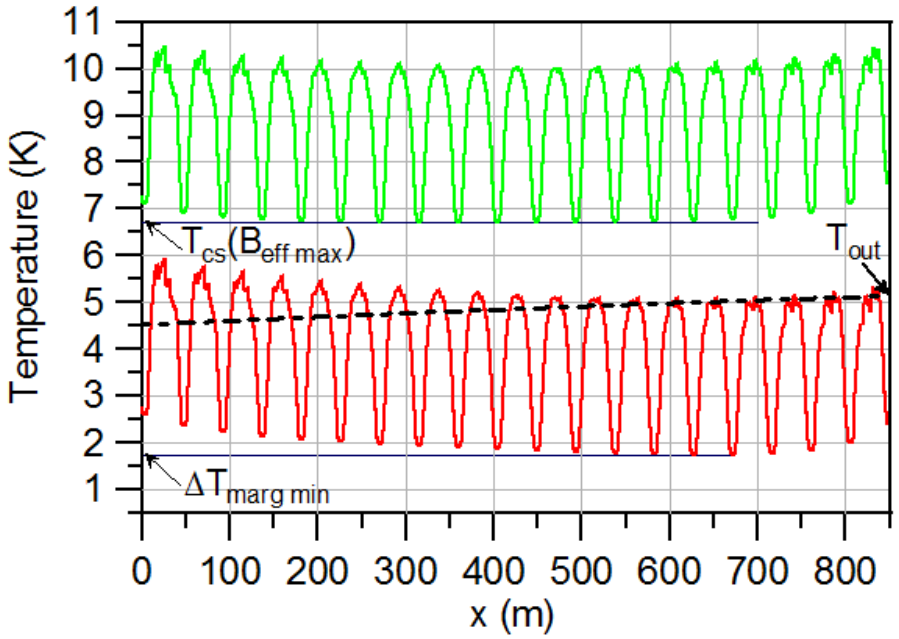

WP#1 L1

Heat load = $= Q_{NH2}+Q_{JR}$

T

T_{cs}

ΔT_{marg}

Very good agreement between the results obtained with THEA and with SM is observed ☺

$$\Delta T_{marg}(x,t) = T_{cs}(x,t) - T_{sc}(x,t)$$

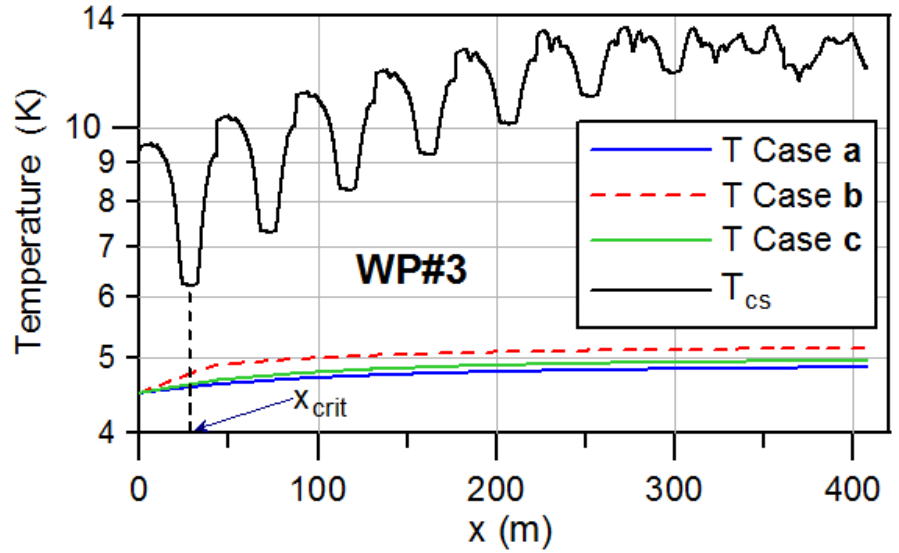

Minimum of ΔT_{marg} in the WP#1 conductors is located at one of the T_{cs} minima in one of the outermost turns, whereas in the WP#3 conductor it is observed at x_{crit} close to the T_{cs} global minimum in the 1st turn

Results – minimum temperature margin evolution in PF coils (CEA design) [14]

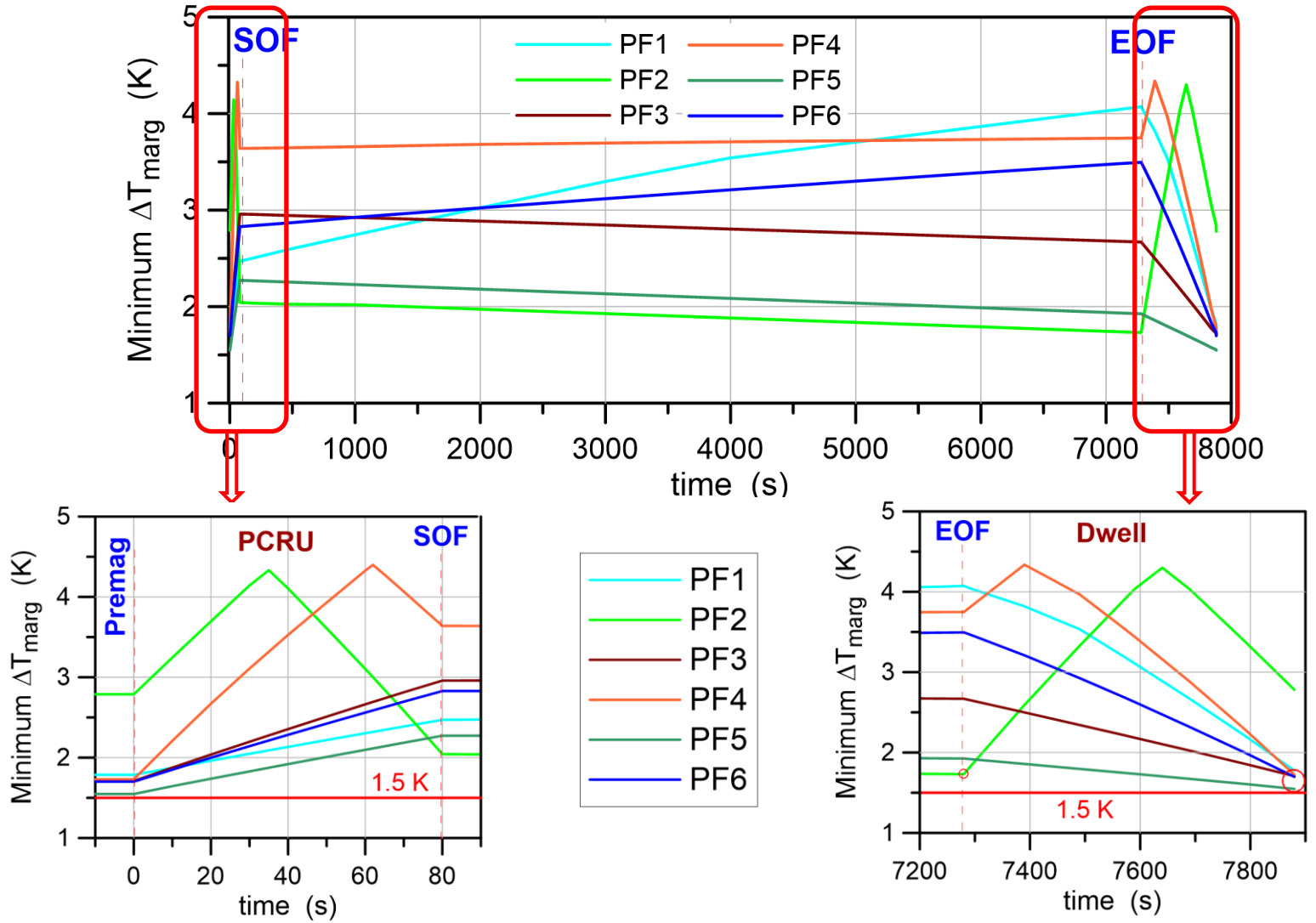

Global minimum of ΔT_{marg} is observed in the very last moment of the current cycle (t = 7880 s) in PF1, PF3-PF6 or at EOF in PF2.

Typical results – quench simulations [14]

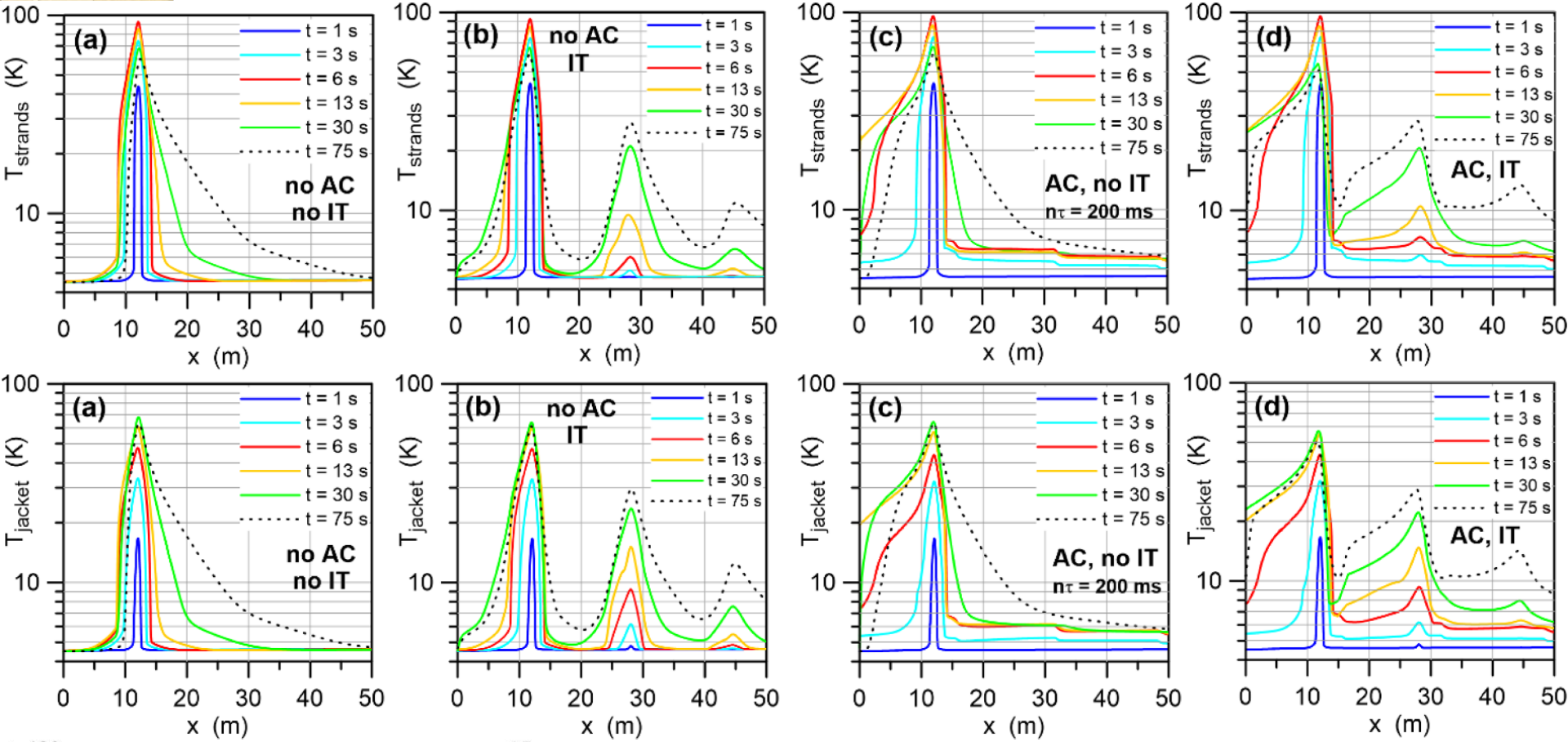

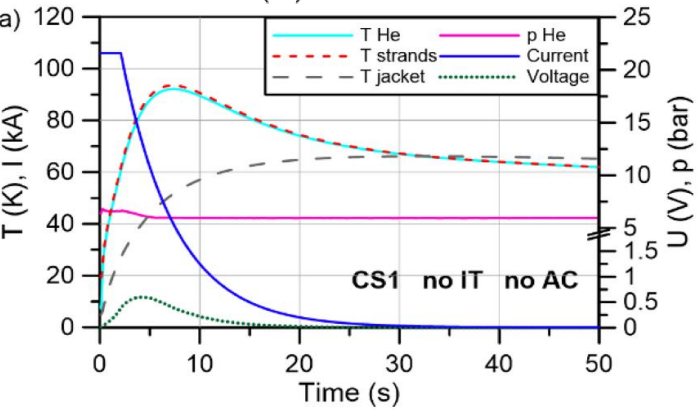

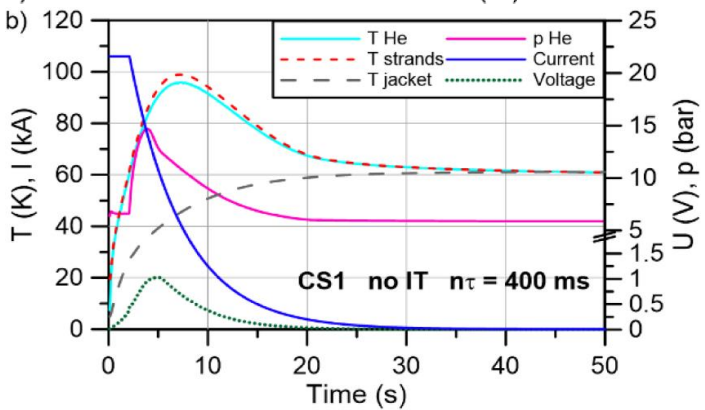

CS1 conductor (CEA design)

THETIS installation

- Progressive cavity pump (BELLIN LZ 500L/KW) with variable speed operation induces pressure head up to 2.5 MPa
- Mass flow rate is precisely adjusted by changing the rotational speed of the pump in the range 10 to 60 Hz or by suitable opening of one of two bypasses of the pump with different diameters.
- A sample is attached to the installation using flexible hose which allows to vary its length.

THETIS installation

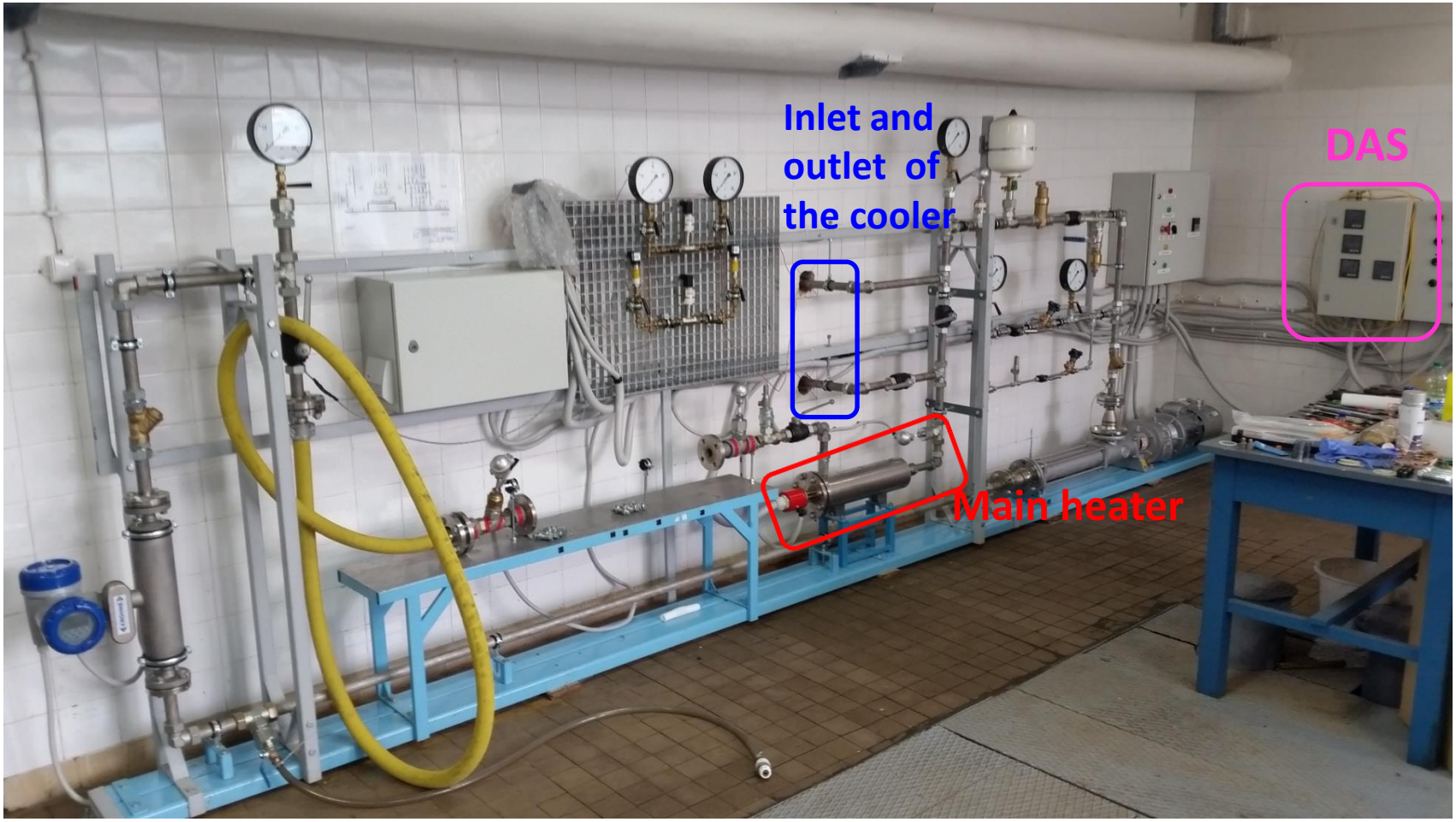

The main heater and the air flow cooler enable adjustments of the water temperature in the circuit in the range from room temperature to about 70°C.

THETIS installation

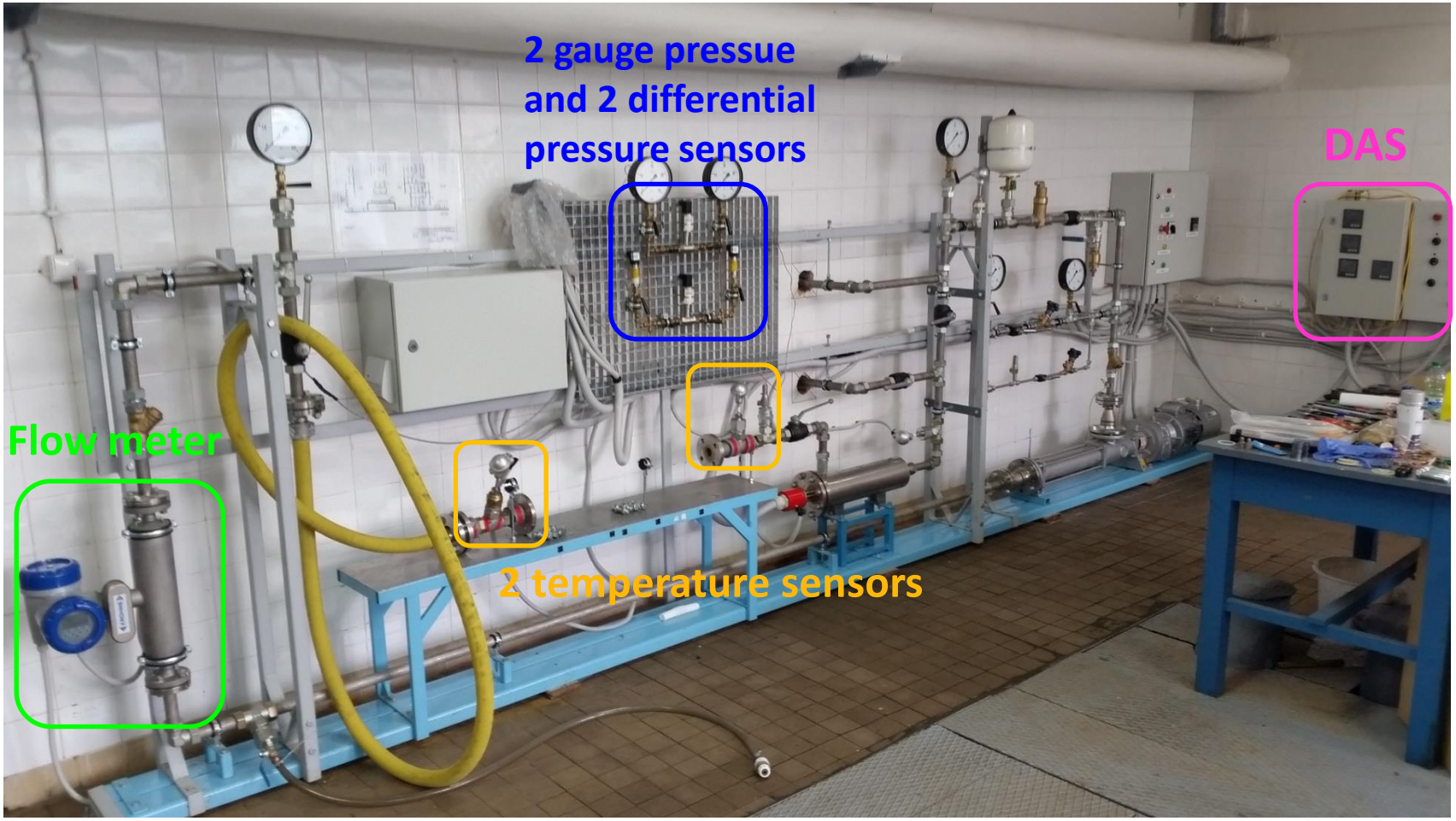

The applied measuring instrumentation and the automatic data acquisition (DAS, four 8-channel data recorders) system enable accurate and convenient measurements.

THETIS – measuring instrumentation

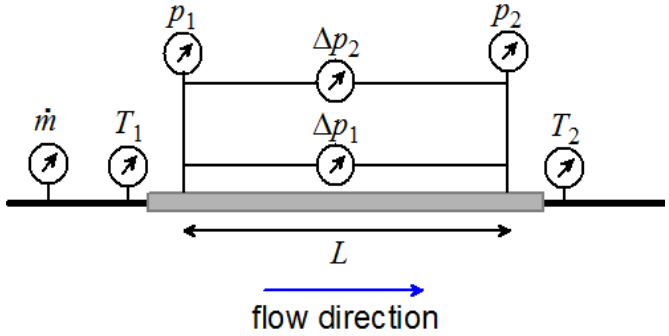

Measuring instrument	Measured quantity	Measuring range	Basic measurement uncertainty
Flow meter	$\dot{m}$	20 – 3000 kg/h	± 0.15% of measured value
Temperature sensor 1 and 2	T_1 , T_2	-200 – 400 ºC	± 0.15 ºC ± 0.2% of |measured value|
Pressure sensor 1	p_1	0 – 2.5 MPa	± 0.2% of measuring range
Pressure sensor 2	p_2	0 -1 MPa	± 0.2% of measuring range
Differential pressure sensor 1	Δp_1	0 – 0.25 MPa	± 0.1% of measuring range
Differential pressure sensor 2	Δp_2	0 – 1.6 MPa	± 0.1% of measuring range
DAS	-	-	± 0.1% of measuring range

$$f = -\frac{2\rho A_{fluid}^3}{\dot{m}^2 P_{wet}} \frac{\Delta p}{L} \qquad \mathrm{Re} = \frac{4\dot{m}}{\mu P_{wet}}$$

water density (ρ) and dynamic viscosity (μ) were calculated at the reference conditions: $p_{ref} = p_{ambient} + (p_1 + p_2)/2$ and $T_{ref} = (T_1 + T_2)/2$.

THETIS – typical example of hydraulic test results

$$\frac{\Delta p}{L} = -\frac{2\rho v^2 f}{D_h} = -\frac{2\dot{m}^2 f}{D_h \rho A_{fluid}^2}$$

$$\mathrm{Re} = \frac{\rho v D_h}{\mu} = \frac{\dot{m} D_h}{\mu A_{fluid}}$$

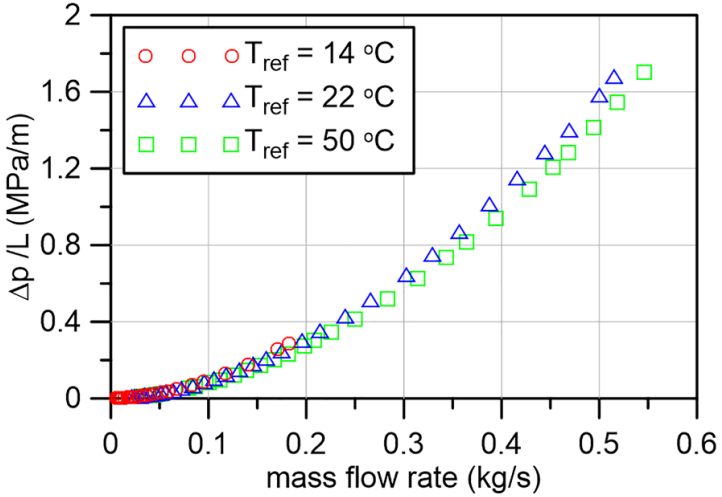

- Data measured at different temperatures, are transformed into the dimensionless form,
- Data in the dimensionless form are grouped at the single trend line, as expected
- The results are well fitted ($R^2 > 0.96$) by the following power law:

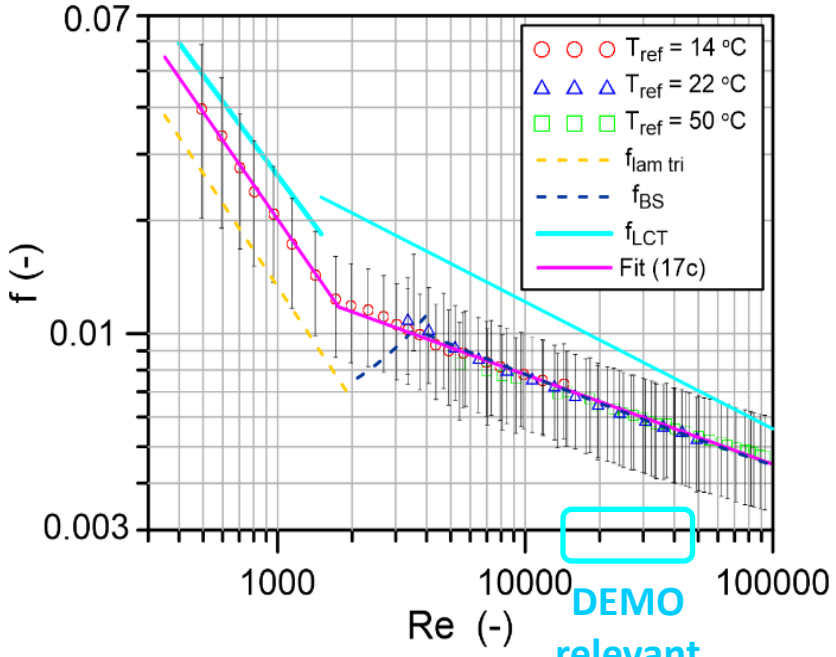

$$f_{Opt3b}(\mathrm{Re}) = \begin{cases} 4.5563 \cdot \mathrm{Re}^{-0.803252} & 300 < \mathrm{Re} < 1750 \\ 0.07005 \cdot \mathrm{Re}^{-0.2386} & 1750 < \mathrm{Re} < 10^5 \end{cases}$$

Summary

- Nuclear fusion seems to be a very promising source of energy for future power plants, but its practical use requires mastering of new technologies. The first fusion power plants are expected in the middle of this century.
- The demand of nuclear fusion reactors for high-current superconducting magnets stimulates significant development of their technology observed in recent years (particularly HTS).
- In recent years we worked on thermal-flow analyzes of superconducting cables (simulations of the conductors' behavior at normal operating conditions and during quench, as well as experimental tests of hydraulic resistance and heat transfer in superconducing cables or dummy samples), in the scope of the EUROfusion WPMAG project.
- We are also involved on analysis and interpretation of the experimental data resulting from the quench experimental campaign on HTS conductors performed at the SULTAN test facility (EPFL-SPC, PSI Villigen, Switzerland)

Thank you for your attention

This work has been carried out within the framework of the EUROfusion Consortium and has received funding from the Euratom research and training programme 2014-2018 and 2019-2020 under grant agreement No 633053. The views and opinions expressed herein do not necessarily reflect those of the European Commission.

This scientific work was partly supported by Polish Ministry of Science and Higher Education within the framework of the scientific financial resources in the years 2014-2020 allocated for the realization of the international co-financed project.

Question Time

Pressure drop in force flow superconducting cables

Pressure drop per unit length of conductor (uncompressible flow):

$$\frac{\Delta p}{L} = -\frac{2\rho v^2 f}{D_h} = -\frac{2\dot{m}^2 f}{D_h \rho A_{fluid}^2}$$

f - **friction factor** (Fanning definition)

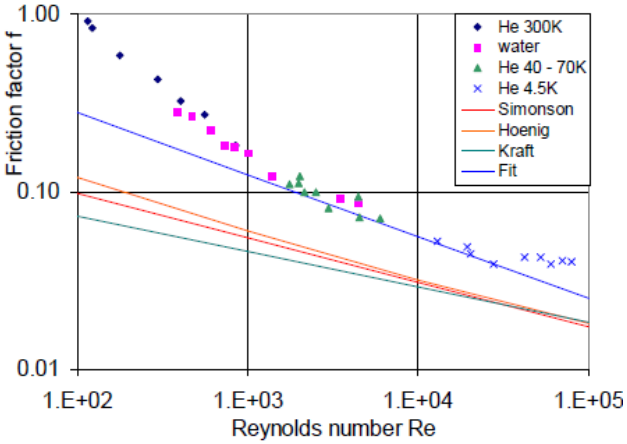

Friction factor correlations for flow in smooth cooling channels

Standard Colburn/McAdams or Bhatti-Shah correlations for the turbulent flow in a straight smooth circular or non-circular duct:

$$f_{Colburn} = 0.046 \cdot \mathrm{Re}^{-0.2} \quad 2 \cdot 10^4 < \mathrm{Re} < 10^6$$

$$f_{BS} = 0.00128 + 0.1143\,\mathrm{Re}^{-0.311} \quad 4000 < \mathrm{Re} < 10^7$$

Friction factor correlations for flow in bundle regions

Two correlations based on a **porous media analogy**:

- $$f_{DF}(\mathrm{Re},\varphi)=\frac{D_h^2\varphi}{2K}\frac{1}{\mathrm{Re}}+\frac{D_h\varphi^2}{2}\frac{C_F}{\sqrt{K}}$$ [5]

$$K=19.6\cdot10^{-9}\varphi^3/(1-\varphi)^2\ \mathrm{m}^2 \qquad C_F/\sqrt{K}=2.42/\varphi^{5.80}\ \mathrm{m}^{-1}$$

- $$f_M(\mathrm{Re},\varphi)=\frac{D_h^2\varphi}{2K}\frac{1}{\mathrm{Re}}+\frac{D_h\varphi^2}{2}\beta\left(\frac{D_h}{\varphi\sqrt{K}}\right)^{0.14}\frac{1}{\mathrm{Re}^{0.14}}$$ [6]

$$K_m=20.9\cdot10^{-9}\varphi^3/(1-\varphi)^2\ \mathrm{m}^2 \qquad \beta=19.1/\varphi^{4.23}\ \mathrm{m}^{-1}$$

- and the Katheder correlation [7]

$$f_{Kath}(\mathrm{Re},\varphi)=\frac{1}{\varphi^{0.72}}\left[\frac{4.875}{\mathrm{Re}^{0.88}}+0.01275\right]$$

where $\varphi=\dfrac{A_{B\ fluid}}{A_{B\,total}}$ is the bundle **void fraction**.

[5] Bagnasco M, Bottura L, Lewandowska M, *Friction factor correlation for CICC's based on a porous media analogy*, Cryogenics 50 (2010) 711–719.

[6] Lewandowska M, Bagnasco M, *Modified friction factor correlation for CICC's based on a porous media analogy*, Cryogenics 51 (2011) 541-545.

[7] Katheder H, *Optimum thermohydraulic operation regime for cable in conduit superconductors (CICS)*, Cryogenics 4 (1994) 595–598, 1994.